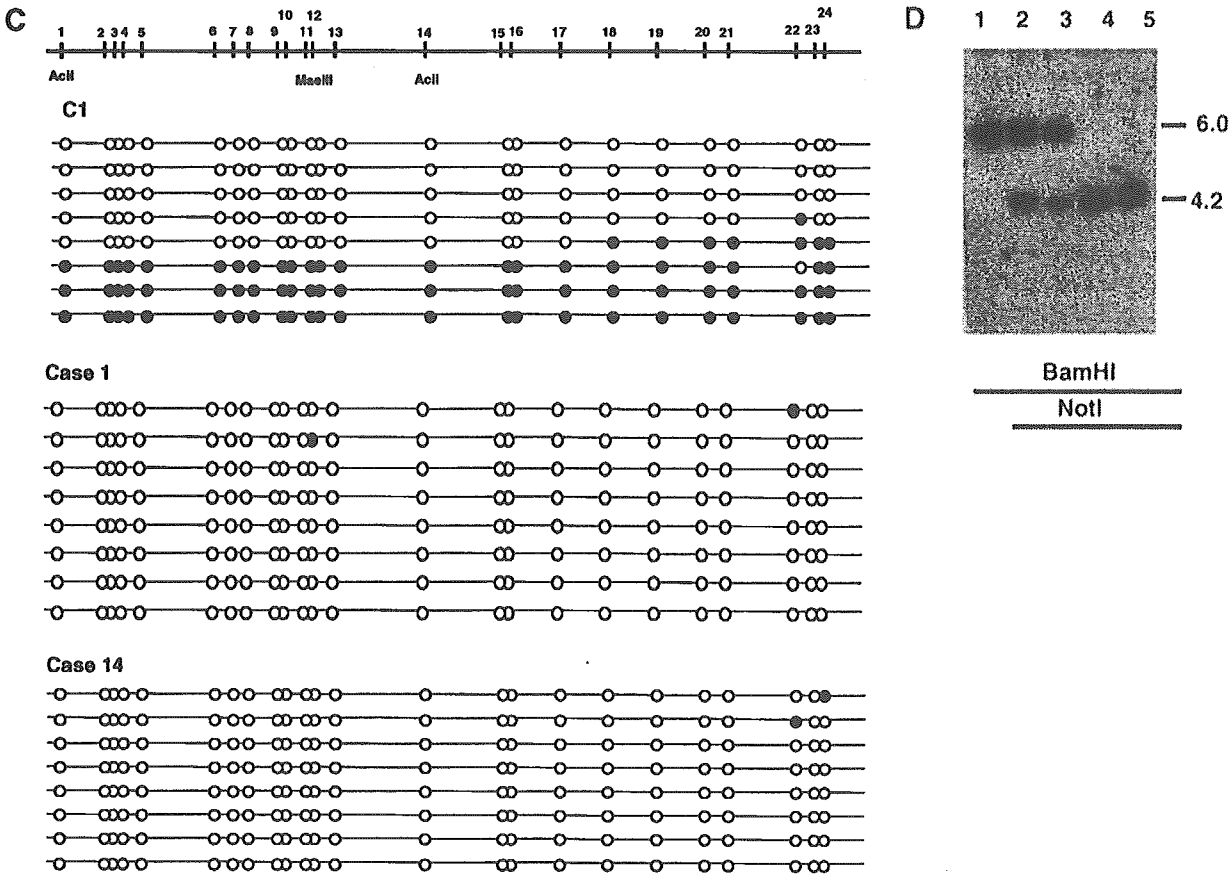

Figure 5. Methylation status of the *ZAC* and *LIT1* CpG islands in BWS and TNDM patients. (**A**) Map of the CpG islands showing the position of the primers used, the methylation sensitive restriction enzyme sites and the predicted product sizes to distinguish between unmethylated (undigested) DNA and methylated (digested) DNA (shown for *ZAC*: AciI; and for *LIT1*: RsaI). (**B**) BWS genomic DNA (top row) is from patients where the methylation status of the *LIT1* CpG island is known: lanes 1–6, unmethylated *LIT1* and lanes 7 and 8, methylated *LIT1*. TNMD genomic DNA (second and third rows) is from previously characterized patients: paternal UPD6 in row 2, lanes 1–7, paternal duplication in row 3, lanes 8–11; and non-UPD/non-duplication in row 3, lanes 12–17. C1 and C2 represent normal controls. All patients with BWS show normal methylation patterns in the *ZAC* CpG island. Two patients with TNDM exhibit an abnormal methylation pattern. (**C**) Bisulfite sequencing analysis (methylation shown as closed circles) showed that 24 CpG sites at the *LIT1* ICR are almost completely unmethylated in 2 TNDM patients (case 1 is paternal UPD6, case 14 has a normal karyotype with an unmethylated ZAC DMR). Case 14 is complicated with umbilical hernia and macroglossia. (**D**) Southern blot analysis of the *LIT1* CpG island in primary leucocyte DNA from the two TNDM patients that showed loss of methylation in the bisulfite assay. The methylation status was analyzed after double digestion with BamHI plus NotI. When the 6.0 kb BamHI fragment encompassing in the *LIT1* CpG island is digested with NotI, a 4.2 kb fragment is produced. Control DNA digested only with BamHI generated a 6.0 kb band (lane 1). Two independent leucocyte DNA samples from normal individuals were found to be a hemi-methylated (lanes 2 and 3). Only the 4.2 kb band is seen in the DNAs from case 1 and case 14 with TNDM confirming loss of DNA methylation (lanes 4 and 5).

ACKNOWLEDGEMENTS

We would like to thank Dr Y. Yoshikawa, Mr Komatsu and Ms H. Hachisu for technical assistance and all members of the laboratory for their support and valuable suggestion. In particular, R. John for the comments on manuscript. This work was supported by a grant from the Ministry of Health and Welfare of Japan and by The 21st Century Program: The Research Core for Chromosome Engineering Technology. Funding to pay the Open Access publication charges for this article was provided by a grant from the Ministry of Health and Welfare of Japan.

Conflict of interest statement. None declared.

REFERENCES

1. McGrath,J. and Solter,D. (1984) Completion of mouse embryogenesis requires both the maternal and paternal genomes. *Cell*, **37**, 179–183.
2. Surani,M.A., Barton,S.C. and Norris,M.L. (1984) Development of reconsituted mouse eggs suggests imprinting of the genome during gametogenesis. *Nature*, **308**, 548–550.
3. Li,E., Bestor,T.H. and Jaenisch,R. (1992) Targeted mutation of the DNA methyltransferase gene results in embryonic lethality. *Cell*, **69**, 915–926.
4. Tilghman,S.M. (1999) The sins of the fathers and mothers: genomic imprinting in mammalian development. *Cell*, **96**, 185–193.
5. Spengler,D., Villalba,M., Hoffmann,A., Pantaloni,C., Houssami,S., Bockaert,J. and Journot,L. (1997) Regulation of apoptosis and cell cycle arrest by *Zac1*, a novel zinc finger protein expressed in the pituitary gland and the brain. *EMBO J.*, **16**, 2814–2825.
6. Kamiya,M., judson,H., Okazaki,H., kusakabe,M., Muramatsu,M., Takada,S., Takagi,N., Arima,T., Wake,N., Kamimura,K. *et al.* (2000) The cell cycle control gene *ZAC/PLAGL1* is imprinted for a strong candidate gene for transient neonatal diabetes. *Hum. Mol. Genet.*, **9**, 433–460.
7. Piras,G., Kharroubi,A.E., Kozlov,S., Escalante-Alcalde,D., Hemandez,L., Copeland,N.G., Gilbert,D.J., jenkins,N.A. and Stewart,C. (2000) *Zac1 (Lot1)*, a potential tumour suppressor gene, and the gene for e-sarcoglycan are maternally imprinted genes; identification by a subtraction screen of novel uniparental fibroblast lines. *Mol. Cell. Biol.*, **20**, 3308–3315.
8. Arima,T., Drewell,R.A., Oshimura,M., Wake,N. and Surani,M.A. (2000) A novel imprinted gene, *HYMAI*, is located within an imprinted domain on human chromosome 6 containing *ZAC*. *Genomics*, **67**, 248–255.

9. Fujii,H., Zhou,W. and Gabrielson,E. (1996) Detection of frequent allelic loss of 6q23–q25.2 in microdissected human breast cancer tissues. *Genes Chromosomes Cancer*, **16**, 35–39.
10. Taguchi,T., Jhanwar,S., Siegfried,J., Keller,S. and Testa,J. (1993) Recurrent deletions of specific chromosomal sites in 1p, 3p, 6q, and 9p in human malignant mesothelioma. *Cancer Res.*, **53**, 4349–4355.
11. Theile,M., Seitz,S., Arnold,W., Jandrig,B., Frege,R., Schlag,P., Haensch,W., Guski,H., Winzer,K-J., Barrett,j. and Scherneck,S. (1996) A defined chromosome 6q fragment (at D6S310) harbors a putative tumor suppressor gene for breast cancer. *Oncogene*, **13**, 677–685.
12. Thrash-Bingham,C.A., Salazar,H., Freed,J.J., Greenberg,R.E. and Tartof,K.D. (1995) Genomic alterations and instabilities in renal cell carcinomas and their relationship to tumor pathology. *Cancer Res.*, **55**, 6189–6195.
13. Abdollahi,A., Godwin,A.K., Miller,P.D., Getts,L.A., Schultz,D.C., Taguchi,T., Testa,J.R. and Hamilton,T.C. (1997) Identification of a gene containing zinc-finger motifs based on lost expression in malignantly transformed rat ovarian surface epithelial cells. *Cancer Res.*, **57**, 2029–2034.
14. Huang,S.-M. and Stallcup,M.R. (2000) Mouse *Zac1*, a transcriptional coactivator and repressor for nuclear receptors. *Mol. Cell. Biol.*, **20**, 1855–1867.
15. May,P. and May,E. (1999) Twenty years of p53 research: structural and functional aspects of the p53 protein. *Oncogene*, **18**, 7621–7636.
16. Kas,K., Voz,M.L., Hensen,K., Meyen,E. and Vande,V.W.J. (1998) Transcriptional activation capacity of the novel PLAG family of zinc finger proteins. *J. Biol. Chem.*, **273**, 23026–23032.
17. Varrault,A., Ciani,E., Apiou,F., Bilanges,B., Hoffmann,A., Pantaloni,C., Bockaert,J., Spengler,D. and Journot,L. (1998) *hZAC* encodes a zinc finger protein with antiproliferative properties and maps to a chromosomal region frequently lost in cancer. *Proc. Natl Acad. Sci. USA*, **95**, 8835–8840.
18. Huang,S-M., Schonthal,A.H. and Stallcup,M.R. (2001) Enhancement of p53-dependent gene activation by the transcriptional coactivator Zac1. *Oncogene*, **20**, 2134–2143.
19. Temple,I.K. and Shield,J.P. (2002) Transient neonatal diabetes, a disorder of imprinting. *J. Med. Genet.*, **12**, 872–875.
20. Arima,T., Drewell,R.A., Arney,K.L., Inoue,J., Makita,Y., Hata,A., Oshimura,M., Wake,N. and Surani,M.A. (2001) A conserved imprinting control region at the *HYMAI/ZAC* domain is implicated in transient neonatal diabetes mellitus. *Hum. Mol. Genet.*, **10**, 1475–1483.
21. Ma,D., Shield,J.P.H., Dean,W., Leclerc,I., Knauf,C., Burcelin,R., Rutter,G.A. and Kelsey,G. (2004) Impaired glucose homeostasis in trangenic mice expressing the human transient neonatal diabetes mellitus locus, TNDM. *J. Clin. Invest.*, **114**, 339–348.
22. Lee,M.P., DeBaun,M.R., Mitsuya,K., Galonek,H.I., Brandenburg,S., Oshimura,M. and Feinberg,A.P. (1999) Loss of imprinting of a paternally expressed transcript, with antisense orientation to KVLQT1, occurs frequently in Beckwith–Wiedemann syndrome and is independent of insulin-like growth factor II imprinting. *Proc. Natl Acad. Sci. USA*, **9**, 5203–5208.
23. Matsuoka,S., Edwards,M.C., Bai,C., Parker,S., Zhang,P., Baldini,A., Harper,J.W. and Elledge,S.J. (1995) $p57^{KIP2}$, a structurally distinct member of the $p21^{CIP1}$ Cdk inhibitor family, is a candidate tumor suppressor gene. *Gen. Dev.*, **9**, 650–662.
24. Hatada,I., Inazawa,J., Abe,T., Nakayama,M., Kaneko,Y., Jinno,Y., Niikawa,N., Ohashi,H., Fukushima,Y., Iida,K. *et al.* (1996) Genomic imprinting of human *p57KIP2* and its reduced expression in Wilms' tumors. *Hum. Mol. Genet.*, **6**, 783–788.
25. Mitsuya,K., Meguro,M., Lee,M.P., Katho,M., Schulz,T.C., Kugoh,H., Yoshida,M.A., Niikawa,N., Feinberg,A.P. and oshimura,M. (1999) *LIT1*, an imprinted antisense RNA in the human *KvLQT1* locus identified by screening for differentially expressed transcripts using monochromosomal hybrids. *Hum. Mol. Genet.*, **8**, 1209–12177.
26. Luo,D.F., Bui,M.M., Muir,A., Maclaren,N.K., Thomson,G. and She,J.X. (1995) Affected-sib-pair mapping of a novel susceptibility gene to insulin-dependent diabetes mellitus (IDDM) on chromosome 6q25-q27. *Am. J. Hum. Genet.*, **57**, 911–919.
27. Rowe,R.E., Wapelhorst,B., Bell,G.I., Risch,N., Spielman,R.S. and Concannon,P. (1995) Linkage and association between insulin-dependent diabetes mellitus (IDDM) susceptibility and markers near the glucokinase gene on chromosome 7. *Nature Genet.*, **10**, 240–242.
28. Shield,J.P.H. (2000) Neonatal diabetes: new insights into aetiology and implications. *Horm. Res.*, **53**, 7–11.
29. Hatada,L., ohashi,H., Fukushima,Y., kaneko,Y., inoue,M., komoto,Y., Okada,A., Ohishi,S., Nabetani,A., Morisaki,H. *et al.* (1996) An imprinted gene *p57 (KIP2)* is mutated in Beckwith–Wiedemann syndrome. *Nature Genet.*, **14**, 171–173.
30. O'Keefe,D., Dao,D., Zhao,L., Sanderson,R., Warburton,D., Weiss,L., A-Yeboa,K. and Tycko,B. (1997) Coding mutations in $p57^{KIP2}$ are present in some cases of Beckwith–Wiedemann syndrome but are rare or absent in Wilms tumors. *Am. J. Hum. Genet.*, **61**, 295–303.
31. Lee,M.P., Hu,R.J., Johnson,L.A. and Feinberg,A.P. (1997) Human *KvLQT1* gene shows tissue-specific imprinting and encompasses Beckwith–Wiedemann syndrome chromosomal rearrangements. *Nature Genet.*, **15**, 181–185.
32. Engel,J.R., Smallwood,A., Harper,A., Higgins,M.J., Oshimura,M., Reik,W., Schofield,P.N. and Maher,E.R. (2000) Epigenotype-phenotype correlations in Beckwith–Wiedemann syndrome. *J. Med. Genet.*, **37**, 921–926.
33. Horiike,S., Mitsuya,K., Meguro,M., Kotobuki,N., Kashiwagi,A., Notsu,T., Schulz,T.C., Shirayoshi,Y. and Oshimura,M. (2000) Targeted disruption of the human *LIT1* locus defines a putative imprinting control element playing an essential role in Beckwith–Wiedemann syndrome. *Hum. Mol. Genet.*, **9**, 2075–2083.
34. Engemann,S., Strodicke,M., Franck,O., Reinhardt,R., Lane,N., Reik,W. and Walter,J. (2000) Sequence and functional comparison in the Beckwith–Wiedemann region: implications for a novel imprinting centre and extended imprinting. *Hum. Mol. Genet.*, **9**, 2691–2706.
35. Fitzpatrick,G.V., Soloway,P.D. and Higgins,M.J. (2002) Regional loss of imprinting and growth deficiency in mice with a targeted deletion of *KvDMR1*. *Nature Genet.*, **3**, 426–431.
36. Sleutels,F., Zwart,R. and Bariow,D.P. (2002) The non-coding *Air* RNA is required for silencing autosomal imprinted genes. *Nature*, **415**, 810–813.
37. Ueoka,Y., Kato,K., Kuriaki,Y., horiuchi,S., Terao,Y., Nishida,J., Ueno,H. and Wake,N. (2000) hepatocyte growth factor modulates motility and invasiveness of ovarian carcinomas via Ras-mediated pathway. *Br. J. Cancer*, **82**, 891–899.
38. Wilkinson,D.G. and Nieto,M.A. (1993) Detection of messenger RNA by *in situ* hybridization to tissue sections and whole mounts. *Methods Enzymol.*, **225**, 361–373.
39. Schreiber,E., Matthias,P., Muller,M.M. and Schaffner,W. (1989) Rapid detection of octamer binding proteins with mini-extracts prepared froma small number of cells. *Nucleic Acids Res.*, **17**, 6419.
40. Westbury,J., Watkins,M., Ferguson-Smith,A.C. and Smith,J. (2001) Dynamic temporal and spatial regulation of the cdk inhibitor $p57^{kip2}$ during embryo morphogenesis. *Mech. Dev.*, **109**, 83–89.
41. Lovicu,F.J. and McAvoy,J.W. (1999) Spatial and temporal expression of $p57^{kip2}$ during murine lens development. *Mech. Dev.*, **86**, 165–169.
42. Mancini-DiNardo,D., Steele,S.J.S., Ingram,R.S. and Tilghman,S.M. (2003) A differentially methylated region within the gene *Kcnq1* functions as an imprinted promoter and silencer. *Hum. Mol. Genet.*, **12**, 283–294.
43. Kanduri,C., Mukhopadhyay,R., Holmgren,C., Kanduri,M. and Thakur,N. (2003) Bidirectional silencing and DNA methylation-sensitive methylation-spreading properties of the *Kcnq1* imprinting control region map to the same regions. *J. Biol.Chem.*, **278**, 9514–9519.
44. Du,M., Beatty,L.G., Zhou,W., Lew,J., Schoenherr,C., Weksberg,R. and Sadowski,P.D. (2003) Insulator and silencer sequences in the imprinted region of human chromosome 11p15.5. *Hum. Mol. Genet.*, **12**, 1927–1239.
45. Constancia,M., Pickard,B., Kelsey,G. and Reik,W. (1998) Imprinting mechanisms. *Genome Res.*, 881–900.
46. Kamikihara,T., Arima,T., Kato,K., Douchi,T., Nagata,Y., Nakao,M. and Wake,N. (2005) Epigenetic silencing of the imprinted gene ZAC by DNA methylation is an early event in the progression of human ovarian cancer. *Int. J. Cancer*, doi:10.1002/ijc.20971.
47. Olek,A. and Walter,J. (1997) The pre-implantation ontogeny of *H19* methylation imprint. *Nature Genet.*, **17**, 275–276.
48. Kaghad,M., Bonnet,H., Yang,A., Creancier,L., Biscan,J.-C., Valent,A., Minty,A., Chalon,P., Lelias,J.-M., Dumont,X. *et al.* (1997) Monoallelically expressed gene related to p53 at 1p36, a region frequently deleted in neuroblastoma and other human cancers. *Cell*, **90**, 809–819.
49. Balint,E., Phillips,A.C., Kozlov,S., Stewart,C.L. and Vousden,K.H. (2002) Induction of $p57^{KIP2}$ expression by p73beta. *Proc. Natl Acad. Sci. USA*, **99**, 3529–3534.

【Beckwith-Wiedemann症候群の分子遺伝学】

Molecular Genetics of Beckwith-Wiedemann Syndrome

副島　英伸・東元　健・向井・常博

Soejima　Hidenobu Higashimoto Ken　Mukai　Tsunehiro

Key words
Beckwith-Wiedemann syndrome, imprinting control region (ICR), differentially methylated region (DMR), DNA methylation, histone H3 lysine 9 methylation

はじめに

Beckwith-Wiedemann症候群(BWS)は，新生児期の臍ヘルニア，巨舌，巨躯を三主徴とする先天奇形症候群で，約10%の患児にWilms腫瘍を含む胎児性腫瘍を合併する。BWSの発症には，ゲノム刷り込みが密接に関わっている。ゲノム刷り込みとは，両親から受け継いだ一対の対立遺伝子（アレル）のうち，由来する親の性に従って片方のアレルのみが優位に発現する現象である。この遺伝子発現パターンは，体細胞では細胞分裂を経て維持される。しかし，生殖細胞形成過程においては一旦消去され，その個体の性に応じた何らかのエピジェネティック（脚注参照）な印が刷り込まれる（刷り込みマーク）。刷り込み遺伝子の多くは特定の染色体領域に集中して存在し，刷り込みドメインを形成しており，刷り込み調節領域(ICR)によりドメインレベルでシスに発現調節されている。ICRが何らかの原因で本来の機能を失うとドメインレベルでの刷り込み遺伝子の発現異常がおこり，疾患が発症する。ICRは，生殖細胞形成過程において刷り込みマークを付加されるが，そのマークとしてはDNAメチル化が最も有力である。一方，最近，アセチル化やメチル化などのヒストン化学修飾が遺伝子発現に重要であると報告され，ICRの刷り込みマークがヒストン修飾である可能性が示唆されている。本項では，BWSの責任領域11p15.5における刷り込みの分子機構について解説する。

1．Beckwith-Wiedemann症候群(BWS)

BWSは，上述の三主徴に加え，低血糖，耳垂の線状溝，内臓腫大，片側肥大などの症状を伴う。合併する腫瘍の60%はWilms腫瘍であり，15%が副腎皮質癌，その他に肝芽腫，横紋筋肉腫などが見られる。85%は孤発例で，15%の家族例は常染色体優性遺伝を示す。孤発例において，①11p15に切断点を持つ母由来の均衡型染色体，②父由来の過剰染色体(11p15部分トリソミー)，③父性片親性ダイソミー(uniparental disomy: UPD)（二本の染色体がどちらも父親由来）を認めるという事実に加え，④家族例では母系遺伝することから，ゲノム刷り込みの関与が示唆されてきた。実際，BWSの遺伝子座11p15.5には数多くの刷り込み遺伝子が存在し，二つのドメインを形成している（図a）。それぞれのドメインは，刷り込み調節領域(ICR)を持ち，独立して刷り込みが制御されている。

2．BWSの分子遺伝学的発症機構

BWSで見られる遺伝子異常とその頻度，および症状との関連を表に示した。ジェネティックな異常は，$p57^{KIP2}$(*KIP2*)の遺伝子変異と11p15.5の転座・重複などであるが，その頻度は低く，BWSの多くはエピジェネティックな異常により発症すると考えられる。最も頻度が高いのは，*KIP2/LIT1*ドメインのICRであるdifferentially methylated region of *LIT1*(*DMR-*

佐賀大学医学部分子生命科学講座分子遺伝学分野：
Division of Molecular Biology and Genetics, Department of Biomolecular Sciences, Saga University Faculty of Medicine
〒849-8501　佐賀市鍋島5-1-1　Fax: 0952-34-2067　E-mail: soejimah@post.saga-med.ac.jp

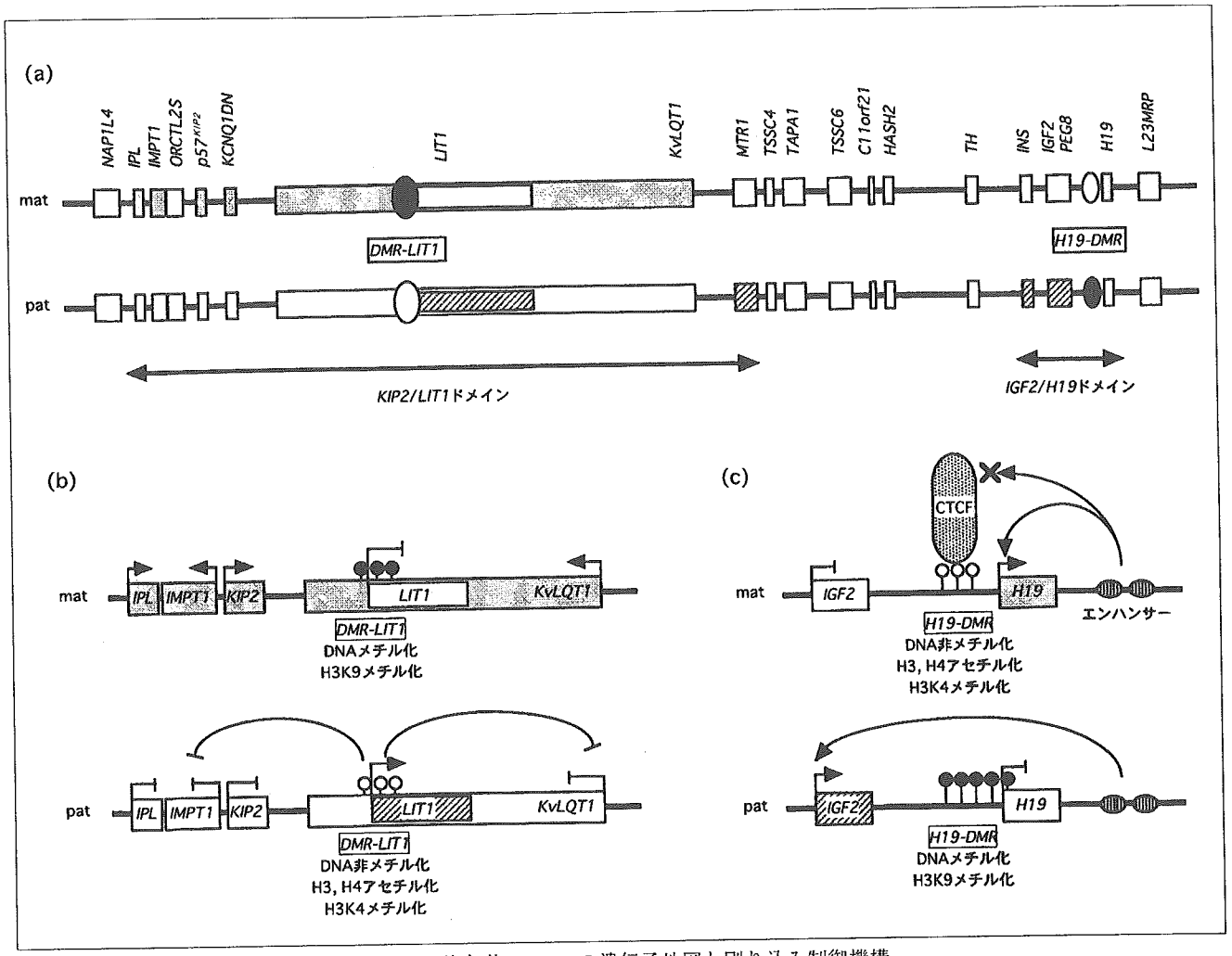

図　ヒト染色体11p15.5の遺伝子地図と刷り込み制御機構

(a) 11p15.5の刷り込みドメイン．楕円はICRを示し，黒はDNAメチル化，白はDNA非メチル化を表す。mat:：母性アレル，pat：父性アレル．□：母性発現，▨：父性発現，□：両アレルとも□の場合は両アレル発現。(b, c) *KIP2/LIT1*ドメインと*IGF2/H19*ドメインの刷り込み調節機構。どちらのドメインについても，母性アレルICRが父型の特徴を獲得することにより，ドメイン内の遺伝子発現パターンも父型となり，BWSの発症につながる。○：非メチル化DNA，●：メチル化DNA

LIT1)の脱メチル化である。父性UPDは，刷り込みドメイン全体のエピジェネティックなマークが父型になるエピジェネティック変異と考えられる。

マウスを用いた研究から，過成長を示す症状は*Igf2*の過剰発現に[1]，臍ヘルニアなどの腹壁欠損は*Kip2*の機能喪失に起因することが示唆された[2]。これは，BWSで見られる*IGF2*の両アレル発現と*KIP2*の遺伝子変異・発現低下に合致する。しかし，両ドメインに同時に異常を認める患者が稀であることや，全く異常が認められない患者が約25%存在することから未知の機序が関与している可能性も否定できない。

3．11p15.5刷り込みドメインの制御機構

1）*KIP2/LIT1*ドメインの刷り込み調節機構（図b）

このドメインのICRは*DMR-LIT1*である。母性アレルの*DMR-LIT1*は，DNAメチル化，ヒストンH3リシン9(H3K9)のメチル化で特徴づけられ，父性アレルは，DNA非メチル化，ヒストンH3とH4のアセチル化，ヒストンH3リシン4(H3K4)のメチル化で特徴づけられる[3]。父性アレル*DMR-Lit1*を欠失させたマウスでは，通常父性アレルでは発現していない刷り込み遺伝子群が発現する[4]。ヒト11番染色体を持つ雑種細胞でも，父性*DMR-LIT1*を欠失させると

表　BWS候補遺伝子の異常と頻度および症状との関連

遺伝子異常または染色体異常		頻度(%)	BWS症状との関連性
*KIP2/LIT1*ドメイン	*DMR-LIT1*の低メチル化	50	腹壁欠損・内臓腫大
	$p57^{KIP2}$の遺伝子変異	～5	臍ヘルニア・巨舌・耳垂線状溝
*IGF2/H19*ドメイン	*H19-DMR*の高メチル化	～10	高発がんリスク
	LOI of *IGF2*	10-15	過成長・巨舌・内臓腫大
刷り込み領域全体	11番染色体父性ダイソミー（父性UPD）	～15	高発がんリスク・低血糖・片側肥大
	11番染色体の異常（転座・重複）	1-2	不明
	異常なし	～25	不明

LOI: loss of imprinting

*KIP2*の発現が回復する[5]。これらの結果は，*DMR-LIT1*がICRであり，父性*DMR-LIT1*が周辺の刷り込み遺伝子をシスに抑制していることを示す。しかし，その詳細な抑制機序は明らかではない。BWSでは，母性アレル*DMR-LIT1*のDNA脱メチル化が最も多く認められる。これにはH3K9の脱メチル化が伴い，さらにH3とH4のアセチル化，H3K4のメチル化がおこる。つまり，母性アレル*DMR-LIT1*が，父型のエピジェネティックな特徴を獲得するのである。この結果，父型になった*DMR-LIT1*が，母性アレルの*KIP2*遺伝子発現を抑制し，発症すると考えられる。事実，*DMR-LIT1*の脱メチル化があるBWS由来の線維芽細胞では*KIP2*の発現が低下している[6]。H3K9のメチル化は，少なくとも刷り込みの維持に必要であることは明らかであり，H3K9メチル化そのものが刷り込みマークである可能性もある。

2）*IGF2/H19*ドメインの刷り込み調節機構（図）

このドメインのICRは，*H19*上流2-5kbにある*H19-DMR*である。母性アレルの*H19-DMR*は，DNA非メチル化，ヒストンH3・H4アセチル化，H3K4メチル化で特徴づけられ，父性アレルは，DNAメチル化，H3K9メチル化で特徴づけられる。母性アレルでは，DNA非メチル化*H19-DMR*にCTCFタンパクが結合してインスレーターとして働く。下流にあるエンハンサーは，インスレーターにブロックされ*IGF2*プロモーターに作用できずに*H19*に作用する。そのため，母性アレルの*IGF2*は発現されず，*H19*が発現する。父性アレルの*H19-DMR*ではDNAメチル化によりCTCFの結合が阻害され，エンハンサーが*IGF2*に作用して父性発現となる[7,8]。DNAメチル化は*H19*プロモーターまでおよび，発現が抑制される。一部のBWSでは母性アレルの*H19-DMR*が高メチル化され，父型の特徴を獲得し，*IGF2*が両アレル発現となる(Loss of imprinting: LOI)。しかし，*H19-DMR*の高メチル化と*IGF2*のLOIが必ずしもリンクするわけでなく，両者を同時に認める症例は少ない。このことは，*H19-DMR*に依存しない*IGF2*のLOIの機序の存在を示唆する。大腸癌では，*IGF2*内にある*DMR*の両アレル低メチル化が*IGF2*のLOIと相関するという報告があり[9]，BWSにおけるLOIの機序の候補として注目される。

4．BWSに合併する腫瘍

BWSに生じる腫瘍の大半はウイルムス腫瘍で，その他に副腎皮質癌，横紋筋肉腫（BWSでは胎児型が多い），肝芽種などが見られる。BWS患児におけるウイルムス腫瘍の危険率は，健常児の800～1000倍高い。これらの胎児性腫瘍では，母性由来11p15.5領域のLOHが認められるため，刷り込みの関与が考えられてきた。

BWSでは，二つの刷り込みドメインのうち，*IGF2/H19*ドメインの異常があると腫瘍発生のリスクが高い（表）。すなわち，*H19-DMR*の高メチル化あるいは父性UPDを示すBWSの24%に腫瘍が発生し，その9割がウイルムス腫瘍である[10]。これは，約70%のウイルムス腫瘍（BWSに伴わない腫瘍も含む）で*IGF2*のLOIが認められ，ほぼ全例に*H19-DMR*の両アレル高メチル化が伴うこととも合致する。さらに，他の胎児性腫瘍においても*H19-DMR*

の高メチル化に伴う*IGF2*のLOIがみられることから，LOIによる*IGF2*の過剰発現が，腫瘍発生に重要であることがわかる。しかし，*IGF2*のLOIを示すBWSで必ずしもウイルムス腫瘍が生じるわけではないので*IGF2*の過剰発現だけでは腫瘍発生に十分ではないと考えられる。

一方，*KIP2/LIT1*ドメインの異常（*DMR-LIT1*の脱メチル化，*KIP2*変異）を示すBWSの腫瘍発生率は5%程度と比較的低い。この場合，ほとんどがウイルムス腫瘍以外の腫瘍である。腫瘍発生とその種類に関して，二つのドメインが異なる関連性を示すことは興味深く，今後の研究課題である。

おわりに

11p15.5に存在する二つのICRにおける刷り込みマークとしては，DNAメチル化とH3K9のメチル化が重要であり，これらは少なくとも刷り込みの維持に必要である。ヒストンリシン残基のメチル化には，付加されるメチル基の数により，モノメチル化，ジメチル化，トリメチル化の3種類があり，さらに，H3K9以外のリシン残基のメチル化が遺伝子発現と関わっているという報告がある。どのリシン残基の何個のメチル化が最も重要なのか，今後の研究により明らかとなるであろう。

最近，卵細胞質精子注入法や体外受精などの生殖補助医療により出生した子供では，BWSを含む刷り込み関連疾患の頻度が高いという報告がされた[11]。このことは，刷り込みマークが，配偶子形成過程だけではなく，受精後も発育段階特異的に印付けされており，細胞を取り巻く環境に作用される可能性を示唆する。刷り込み機構の観点からは興味深い事象である。

刷り込みに代表されるエピジェネティクスは，ゲノムDNAに書かれている遺伝情報を，適切な時期に，適切な量だけ発現させて，様々な生命現象を調節している。エピジェネティクス研究は，ポストシークエンス時代の重要な研究分野であり，ますます発展すると考えられる。

謝　辞

本項執筆の機会を与えていただきました，秦　順一先生に感謝致します。

脚　注

エピジェネティクス：DNAの配列の変化を伴わずに遺伝子機能を調節する機構の総称。具体的には，DNAのメチル化やゲノムDNAに接触するヒストンなどのクロマチンタンパクの化学修飾のことを指す。これらの修飾は，可逆的で複雑な情報のシステムを作り上げており，エピジェネティックな情報がゲノムに書かれた遺伝情報の発現を操っている。

文　献

1) Sun F L, Dean W L, Kelsey G, *et al.*: Transactivation of *Igf2* in a mouse model of Beckwith-Wiedemann syndrome. Nature. 389: 809-815, 1997.
2) Zhang P, Liegeois N J, Wong C, *et al.*: Altered cell differentiation and proliferation in mice lacking *p57^{KIP2}* indicates a role in Beckwith-Wiedemann syndrome. Nature. 387: 151-158, 1997.
3) Higashimoto K, Urano T, Sugiura K, *et al.*: Loss of CpG methylation is strongly correlated with loss of histone H3 lysine 9 methylation at *DMR-LIT1* in patients with Beckwith-Wiedemann syndrome. Am. J Hum Genet. 73: 948-956, 2003.
4) Fitzpatrick G V, Soloway P D, Higgins M J,: Regional loss of imprinting and growth deficiency in mice with a targeted deletion of *KvDMR1*. Nat Genet. 32: 426-431, 2002.
5) Horike S, Mitsuya K, Meguro M, *et al.*: Targeted disruption of the human *LIT1* locus defines a putative imprinting control element playing an essential role in Beckwith-Wiedemann syndrome. Hum Mol Genet. 9: 2075-2083, 2000.
6) Diaz-Meyer N, Day C D, Khatod K, *et al.*: Silencing of CDKN1C (*p57^{KIP2}*) is associated with hypomethylation at *KvDMR1* in Beckwith-Wiedemann syndrome. J Med Genet. 40: 797-801, 2003.
7) Bell A C, Felsenfeld G,: Methylation of a CTCF-dependent boundary controls imprinted expression of the *Igf2* gene. Nature. 405: 482-485, 2000.
8) Hark AT, Schoenherr, C J, Katz D J, *et al.*: CTCF mediates methylartion-sensitive enhancer-blocking activity at the *H19/Igf2* locus. Nature. 405: 486-489, 2000.
9) Cui H, Onyango P, Brandenburg S, *et al.*: Loss of imprinting in colorectal cancer linked to hypomethylation of *H19* and *IGF2*. Cancer Res. 62: 6442-6446, 2002.
10) Weksberg R, Nishikawa J, Caluseriu O, *et al.*: Tumor development in the Beckwith-Wiedemann syndrome is associated with a variety of constitutional molecular 11p15 alterations including imprinting defects of KCNQ1OT1. Hum Mol Genet. 10: 2989-3000, 2001.
11) DeBaun M R, Niemitz E L, Feinberg A P,: Association of *in vitro* fertilization with Beckwith-Wiedemann syndrome and epigenetic alterations of *LIT1* and *H19*. Am J Hum Genet. 72: 156-160, 2003.

CE: xxx ED: Sathya Op: Srini PAS:200215

ORIGINAL ARTICLE

Generation of the Novel Monoclonal Antibody Against TLS/EWS-CHOP Chimeric Oncoproteins That Is Applicable to One of the Most Sensitive Assays for Myxoid and Round Cell Liposarcomas

Kosuke Oikawa, PhD, Tsuyoshi Ishida, MD,† Tetsuo Imamura, MD,⊥ Keiichi Yoshida, MS,* Masakatsu Takanashi, PhD,§ Hiroyuki Hattori, MD,‡ Akio Ishikawa,* Koji Fujita,* Kengo Yamamoto, MD,‡ Jun Matsubayashi, MD,¶ Masahiko Kuroda, MD,* and Kiyoshi Mukai, MD¶*

Abstract: The fusion oncoproteins, TLS-CHOP and EWS-CHOP, are characteristic markers for myxoid and round cell liposarcomas (MLS/RCLS). Especially, the peptide sequence of 26 amino acids corresponding to the normally untranslated *CHOP* exon 2 and parts of exon 3 (5′-UTR) is a unique structure for these chimeric proteins. In this report, we have generated monoclonal antibodies against the unique peptide sequence of TLS/EWS-CHOP oncoproteins. These antibodies reacted with TLS-CHOP fusion protein, but not reacted with normal TLS and CHOP proteins by Western blot analysis. In addition, one of the antibodies also recognized the chimeric oncoprotein in archival paraffin-embedded tissue samples of MLS/RCLS. The oncoprotein was detectable by the antibody even in the paraffin-embedded tissue samples whose mRNAs were too degraded to be detected by a nested reverse transcription-polymerase chain reaction-based assay. Thus, the molecular assay using the novel antibody is expected to be one of the most sensitive diagnostic assays for MLS/RCLS.

Key Words: myxoid liposarcoma, round cell liposarcoma, TLS-CHOP, monoclonal antibody, immunohistochemistry

(*Am J Surg Pathol* 2006;00:00–00)

All of known human myxoid and round cell liposarcomas (MLS/RCLS) are associated with chromosomal translocations.[18] These chromosomal translocations lead to gene fusions that encode chimeric oncoproteins consisting of an N terminus contributed by one of two related genes, *TLS* (also known as *FUS*) or *EWS*, and a C terminus contributed by the *CHOP* (also called *GADD153*) gene.[3,16,19] Both components of the resulting fusion oncoproteins are important to its transforming activity.[10,20]

These *TLS/EWS* and *CHOP* gene fusions are useful for the precise diagnosis of MLS/RCLS.[1,4,6,8,15] Various techniques, including conventional cytogenetics, Southern blotting , fluorescent in situ hybridization, and reverse transcription-polymerase chain reaction (RT-PCR), have been used to identify these lesions.[12] Especially, RT-PCR is the most widely used approach because of its specificity and sensitivity for detection of the fusion gene transcripts. It is easy in general to amplify the cDNA fragment derived from the fusion gene transcripts in fresh or snap-frozen tissue samples. Amplification of cDNA fragments from RNAs in formalin-fixed, paraffin-embedded tissue samples is, however, sometimes terribly difficult because RNAs in these tissue samples are often shortened by their degradation. Furthermore, TLS/EWS-CHOP chimeric genes have structural diversity, and we have to carefully choose the primer combination for RT-PCR to detect the chimeric genes.

In this report, we have generated novel monoclonal antibodies specific for TLS/EWS-CHOP oncoproteins. Immunohistochemical analysis using one of the antibodies was more sensitive than the nested RT-PCR for detection of the *TLS-CHOP* transcripts or its gene products in paraffin-embedded tissue samples. Thus, we expect that the antibody has a great advantage for molecular diagnosis of MLS/RCLS.

MATERIALS AND METHODS

Antibody Preparation and Western Blotting

To generate monoclonal antibodies specific for TLS-CHOP chimeric protein, we synthesized an oligo-

From the Departments of *Pathology; and ‡Orthopedic Surgery and ¶Diagnostic Pathology, Tokyo Medical University, Tokyo, Japan; †Department of Pathology, Kanto Medical Center NTT-EC, Tokyo, Japan; §National Research Institute for Child Health and Development, Tokyo, Japan; and ⊥Department of Surgical Pathology, Faculty of Medicine, Teikyo University, Tokyo, Japan.

Supported in part by Grants-in-Aid from the Ministry of Education, Culture, Sports, Science and Technology of Japan, the Ministry of Health, Labour and Welfare of Japan, and Japan Health Sciences Foundation.

Reprints: Masahiko Kuroda, MD, Department of Pathology, Tokyo Medical University, 6-1-1 Shinjuku, Shinjuku-ku, Tokyo, 160-8402, Japan (e-mail: kuroda@tokyo-med.ac.jp).

peptide (FKKEVYLHTSPHLKADVLFQTDPTAE) corresponding to the amino acids 268 to 293 of TLS-CHOP (type I) fusion protein. The region is specifically translated from the normally untranslated exon 2 and parts of exon 3 of *CHOP* when *TLS* and *CHOP* are formed: the chimeric oncogene. We then immunized mice against the oligopeptide. Spleen cells of an immunized mouse were fused with P3UI mouse myeloma cells as described previously.[7] Of the 159 hybrids generated, two clones showed exclusive reactivity with TLS-CHOP by ELISA. Immunoblot analyses were performed as previously described.[13] Anti-FUS/TLS (H-76) rabbit polyclonal antibody (Santa Cruz Biotechnology, Santa Cruz, CA; sc-25540) and anti-GADD153 (B-3) mouse monoclonal antibody (Santa Cruz; sc-7351) were purchased. The anti-TLS-CHOP monoclonal antibodies were used at a dilution of 1:2500, and antibodies against TLS and CHOP (GADD153) were used at a dilution of 1:200.

Cell Culture, Chemicals, and Vector Transfection

NIH 3T3 cells were obtained from ATCC and were grown as previously described.[14] Tunicamycin (Sigma) was prepared in dimethyl sulfoxide (DMSO) and used at 2 μg/mL for 8 hours.

To create an expression vector encoding *TLS-CHOP*, cDNA fragment containing the complete coding region of *TLS-CHOP* (type 1) was amplified by PCR using the primers 5′-CGGACATGGCCTCAAACG-3′ and 5′-TGTTCATGCTTGGTGCAG-3′, and inserted into the mammalian expression vector, pcDNA3.1(−) (Invitrogen). NIH3T3 cells were then transfected with the TLS-CHOP expression vector using Lipofectamine 2000 reagent (Invitrogen) and incubated for 24 hours.

Tumor Samples

Tissue samples were fixed in 20% formalin, embedded in paraffin, and stained with hematoxylin and eosin. The tumor samples used in this study were as follows: 16 myxoid liposarcomas (MLS), 5 mixed-type liposarcomas (myxoid with round cell areas) (MLS+RCLS), 2 round cell liposarcomas (RCLS), 2 well-differentiated liposarcomas (WD-LS), 2 pleomorphic liposarcomas (P-LS), 4 myxoid type malignant fibrous histiocytomas (MFH m-type), 4 storiform-pleomorphic type malignant fibrous histiocytomas (MFH s-p type), 2 leiomyosarcomas (LMS), 1 embryonal rhabdomyosarcoma (E-RMS), 2 monophasic fibrous-type synovial sarcomas (SS mf-type), 2 malignant peripheral nerve sheath tumors (MPNST), and 4 Ewing's sarcoma/primitive neuroectodermal tumors (PNET) (Tables 1, 2). All of these tumor samples were diagnosed by detailed histopathologic observation.

RNA Isolation, RT-PCR, and Immunohistochemical Analysis

Total RNA from formalin-fixed, paraffin-embedded tumor samples was extracted using ISOGEN PB Kit (Nippon gene, Tokyo, Japan). First-strand cDNA synthesis was performed as previously described.[9] We then performed nested PCR as described.[4] An aliquot of the second PCR product was fractionated by electrophoresis on a 2% agarose gel and stained with ethidium bromide. The quality of tumor RNAs was assessed by amplification

TABLE 1. Clinical and Molecular Findings of Myxoid and Round Cell Liposarcoma in This Study

Case	Location	Age(yr)/Sex	Histology	Tumor size (cm)	PCR		IHC
					TLS-CHOP	*PGK*	TLS/EWS-CHOP
1	rt thigh	76/F	MLS	5 × 2.5 × 1	–	–	+
2	rt lower leg	35/M	MLS+RCLS	13 × 5 × 5	type 2	+	+
3	lt thigh	50/M	MLS		type 2	+	+
4	rt buttock	53/M	MLS+RCLS	17 × 11 × 9	type 2	+	+
5	rt thigh	51/M	MLS	30 × 15 × 15	–	–	+
6	lt thigh	33/M	RCLS	9.5 × 9.5 × 9.5	type 2	+	+
7	lt popliteal	68/M	MLS	10 × 10 × 10	nd	nd	+
8	lt thigh	37/F	MLS	4.5 × 4.5 × 4.5	nd	nd	+
9	lt thigh	40/F	MLS+RCLS	5.2 × 5.2 × 5.2	nd	nd	+
10	lt thigh	32/M	MLS	9 × 9 × 9	nd	nd	+
11	lt inguinal	47/F	MLS	6 × 6 × 6	nd	nd	+
12	lt popliteal	19/F	MLS	7 × 7 × 7	nd	nd	+
13	lt thigh	29/F	RCLS	3.9 × 3.9 × 3.9	nd	nd	+
14	lt arm	65/M	MLS	unidentified	nd	nd	+
15	lt thigh	80/M	MLS	19 × 19 × 19	nd	nd	+
16	retroperitoneum	59/F	MLS	unidentified	nd	nd	+
17	rt inguinal	40/F	MLS	8 × 8 × 8	nd	nd	+
18	rt thigh	55/F	MLS	12 × 12 × 12	nd	nd	+
19	rt thigh	61/M	MLS	17 × 17 × 17	nd	nd	+
20	rt thigh	34/M	MLS	11 × 11 × 11	nd	nd	+
21	back	50/M	MLS	14 × 14 × 14	nd	nd	+
22	lt inguinal	62/F	MLS+RCLS	5.5 × 5.5 × 5.5	nd	nd	–
23	lt thigh	64/F	MLS+RCLS	9 × 9 × 9	nd	nd	–

MLS, myxoid liposarcoma; RCLS, round cell liposarcoma; nd, not determined.

TABLE 2. Clinical, Histological, and Molecular Findings of Tumors in This Study Except for MLS/RCLS

Case	Location	Age(yr)/Sex	Histology	Tumor size (cm)	PCR		IHC
					TLS-CHOP	*PGK*	TLS/EWS-CHOP
24	mediastinum	20/M	PNET	5 × 4.5 × 2.5	–	+	–
25	mediastinum	24/M	PNET	unidentified	nd	nd	–
26	thigh	40/F	PNET	3 × 3 × 3	nd	nd	–
27	back	32/F	PNET	3.5 × 3.5 × 3.5	nd	nd	–
28	lt thigh	48/F	WD-LS	12 × 9.5 × 3.5	–	–	–
29	lt thigh	72/F	WD-LS	7 × 4.5 × 3.5	–	+	–
30	rt buttock	62/M	P-LS	6 × 5 × 5	–	+	–
31	retroperitoneum	46/M	P-LS	unidentified	nd	nd	–
32	rt back	82/M	MFH s-p type	15 × 9 × 3.5	–	–	–
33	rt thigh	77/F	MFH m-type	11 × 6 × 1	–	+	–
34	lt knee	69/M	MFH s-p type	2.8 × 2.8 × 2.8	nd	nd	–
35	rt thigh	62/F	MFH m-type	5 × 5 × 5	nd	nd	–
36	rt arm	85/F	MFH s-p type	unidentified	nd	nd	–
37	lt lower leg	46/M	MFH m-type	6 × 6 × 6	nd	nd	–
38	lt thigh	49/M	MFH s-p type	21 × 21 × 21	nd	nd	–
39	lt thigh	78/M	MFH m-type	9 × 9 × 9	nd	nd	–
40	uterus	51/F	LMS	9.5 × 9.5 × 9.5	nd	nd	–
41	pelvic cavity	74/M	LMS	13 × 13 × 13	nd	nd	–
42	left foot	48/F	E-RMS	10.5 × 10.5	nd	nd	–
43	forearm	26/F	SS mf-type	unidentified	nd	nd	–
44	thigh	46/F	SS mf-type	13 × 13 × 13	nd	nd	–
45	cheek	46/M	MPNST	3.3 × 3.3 × 3.3	nd	nd	–
46	shoulder	11/M	MPNST	26 × 26 × 26	nd	nd	–

PNET, Ewing's sarcoma/primitive neuroectodermal tumor; WD-IPS, well-differentiated liposarcoma; MFH m-type, myxoid type of malignant fibrous histiocytoma; MFH s-p type, storiform-pleomorphic type of malignant fibrous histiocytoma; LMS, leiomyosarcoma; E-RMS, embryonal rhabdomyosarcoma; SS mf-type, monophasic fibrous type synovial sarcoma; MPNST, malignant peripheral nerve sheath tumor; nd, not determined.

of a 247-basepair portion of the ubiquitously expressed phosphoglycerate kinase (PGK) transcript as described.[2]

Standard indirect immunoperoxidase procedures were used for immunohistochemistry (LSAB2 Kit, DakoCytomation, Kyoto, Japan). After microwave pretreatment for antigen retrieval, an anti-TLS-CHOP monoclonal antibody was applied at a dilution of 1:800. Diaminobenzidine was used as the chromogen.

RESULTS

Generation of Anti-TLS/EWS-CHOP Antibodies

To generate monoclonal antibodies specific for TLS/EWS-CHOP oncoproteins, we selected the 26-amino acid oligopeptide from TLS/EWS-CHOP chimeric proteins that corresponds to the normally untranslated *CHOP* exon 2 and parts of exon 3 (5′-UTR) as the antigen (Fig. 1A). We then obtained two clones of anti-TLS/EWS-CHOP monoclonal antibodies. To confirm the specificity of these antibodies, we performed Western blot analysis with total cell lysates from NIH3T3 cells transfected with a TLS-CHOP expression vector or treated with Tunicamycin. Tunicamycin treatment induces CHOP expression.[21] As shown in Figure 1B, anti-TLS/EWS-CHOP antibodies reacted with TLS-CHOP oncoprotein but not with both normal TLS and CHOP proteins (Fig. 1B). Normal TLS and CHOP signals were shown with anti-TLS and anti-CHOP antibodies, respectively. These data indicated that the anti-TLS/EWS-CHOP antibodies specifically recognized TLS-CHOP fusion oncoprotein.

Detection of *TLS-CHOP* Fusion Transcripts in Myxoid and Round Cell Liposarcomas in Paraffin-Embedded Tissues

Our final goal of this study is to establish the most reliable and usable molecular assay for diagnosis of MLS/RCLS. Previously, Hisaoka et al reported that a nested RT-PCR-based assay could be applied to paraffin-embedded tissues to detect the *TLS-CHOP* gene transcripts as a diagnostic aid for MLS/RCLS.[4] Thus, we first examined paraffin-embedded sarcoma tissue samples obtained in this study by the nested RT-PCR-based assay. Because RNAs were not obtained from many tissue samples available in this study, we examined *TLS-CHOP* expression in only 12 cases. We also assayed PGK transcripts in the samples to assess the quality of their mRNAs because the *PGK* gene is ubiquitously expressed. We detected *TLS-CHOP* transcripts in 4 (67%) of 6 paraffin-embedded samples of MLS/RCLS (Table 1). The nucleotide sequences of the nested RT-PCR products were confirmed by sequence analysis. We did not identify the *PGK* gene products in the other two MLS/RCLS samples without detectable *TLS-CHOP* transcripts, suggesting that the quality of the mRNAs were insufficient for the nested RT-PCR. We did not detect *TLS-*

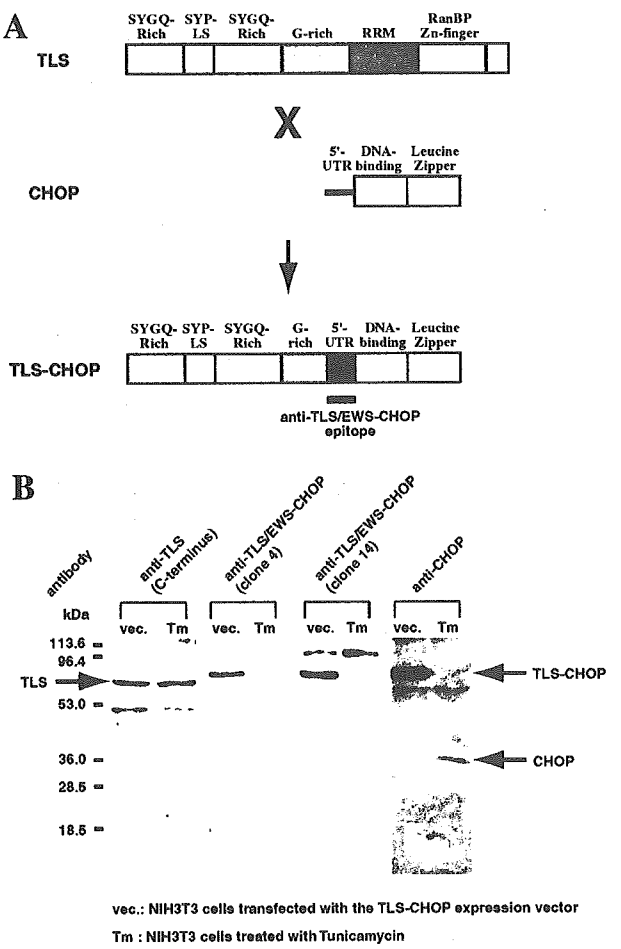

FIGURE 1. Specification of the novel anti TLS/EWS-CHOP antibodies. A, Schematic structures of TLS, CHOP, and TLS-CHOP proteins. Fusion of TLS with CHOP results in a chimeric protein where the C-terminus domains of TLS are replaced by CHOP. The peptide sequence corresponding to the normally untranslated region (5′-UTR) is expressed in the fusion protein. The recognition site of the novel monoclonal antibodies is indicated as "anti-TLS/EWS-CHOP epitope." B, Western blot analysis of TLS-CHOP protein with the total extracts from NIH3T3 cells transfected with TLS-CHOP expression vector (vec) and NIH3T3 cells expressing CHOP induced by Tunicamycin treatment (Tm) using the novel anti TLS/EWS-CHOP monoclonal antibodies. Signals of TLS and CHOP proteins were also shown by Western blot analysis using the anti-TLS (C-terminus) polyclonal antibody and the anti-CHOP monoclonal antibody, respectively.

CHOP transcripts in the tumor tissue samples except for MLS/RCLS, although *PGK* transcripts were detected in all of these tumor samples except for one myxoid variant of malignant fibrous histiocytoma (MFH) and one well-differentiated liposarcoma (WD-LS) (Table 2).

Detection of TLS/EWS-CHOP Fusion Protein by Immunohistochemistry

We next examined whether the newly generated anti-TLS/EWS-CHOP monoclonal antibodies recognize TLS/EWS-CHOP fusion proteins in paraffin-embedded MLS/RCLS tissue samples or not. We performed immunohistochemical analysis using one of the antibodies, anti-TLS/EWS-CHOP antibody (clone 14), and observed nuclear staining of tumor cells in almost all cases (21 of 23 cases; 91%) of MLS/RCLS containing the samples without detectable TLS-CHOP transcripts by the nested RT-PCR (Table 1; Fig. 2A–F). The antibody reacted with tumor cells. Neither normal adipocytes nor endothelial cells of blood vessel were recognized. On the other hand, we did not detect positive nuclear staining in MFH, WD-LS, P-LS, LMS, E-RMS, SS, MPNST, and PNET samples (Table 2; Fig. 2G–J). Slight background staining was also observed in cytoplasm of muscle tissue cells (data not shown). However, it was easy to distinguish the background staining from TLS/EWS-CHOP-positive staining because of their localizations. This background signal may correspond to the 100-kDa protein reacted with the antibody (clone 14) by Western blot analysis (Fig. 1B). TLS/EWS-CHOP antibody (clone 4) failed to detect TLS-CHOP in all cases of paraffin-embedded tissue samples.

DISCUSSION

The *TLS/EWS-CHOP* fusion genes are characteristic for MLS/RCLS. Most of human MLS/RCLS are associated with the specific chromosomal translocations that led to these gene fusions.[8] Thus, these chimeric genes or their gene products are expected to be useful diagnostic molecular markers for diagnosis of MLS/RCLS. There are, however, several structural variants of the *TLS/EWS-CHOP* fusion genes as shown in Fig. 3.[5] In this report, we have generated novel monoclonal antibodies, anti-TLS/EWS-CHOP antibodies (clones 4 and 14), against the normally untranslated *CHOP* exon 2 and parts of exon 3 (5′-UTR). The antibodies are expected to recognize every variant form of TLS/EWS-CHOP except for TLS-CHOP type 4 (Fig. 3). In addition, the anti-TLS/EWS-CHOP antibody (clone 14) is able to detect the fusion oncoproteins even in paraffin-embedded tissue samples of MLS/RCLS (Fig. 2B, D, E). Thus, the non-positive-stained cases (case nos. 22 and 23) of MLS/RCLS by immunohistochemistry using the antibody (clone 14) (Table 1) may have TLS-CHOP type 4, although their subtypes were not confirmed because their RNAs were unavailable. The undetectable TLS-CHOP type 4 is, however, only a small portion (2.5%) of the whole MLS/RCLS cases (Table 3).[4–6,8,16,17] Therefore, the novel anti-TLS/EWS-CHOP antibody (clone 14) may become a strong tool for diagnosis of MLS/RCLS.

TLS/EWS-CHOP play important role in the oncogenesis of MLS/RCLS.[9,11] Although the mechanism of oncogenesis by TLS/EWS-CHOP is not fully understood, the chimeric oncoproteins are thought to induce un-

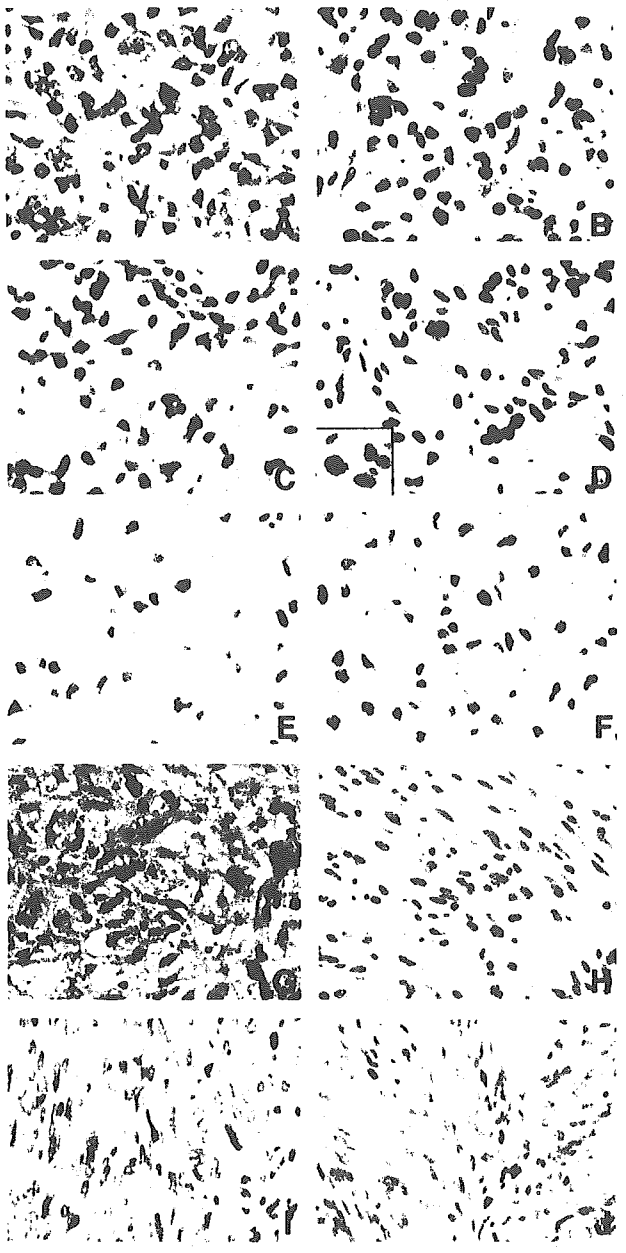

FIGURE 2. Immunohistochemical analysis using anti TLS/EWS-CHOP antibody (clone 14) (original magnification ×400). A, C, E, G, and I, Hematoxylin and eosin staining. B, D, F, H, and J, TLS/EWS-CHOP immunostaining. A, B, MLS+RCLS (case no. 2) shows uniform round cell proliferation and nuclear immunostaining for TLS-CHOP in tumor cells. MLS (case no. 3) (C, D) and MLS (case no. 1) (E, F) show proliferation of lipoblasts with plexiform capillary network and myxoid material, and nuclear immunostaining for TLS-CHOP in tumor cells. D (inset), TLS-CHOP expression in mitotic cells. P-LS (case no. 9) (G, H) and LMS (case no. 41) (I, J) show proliferation of undifferentiated cells, and no positive immunostaining.

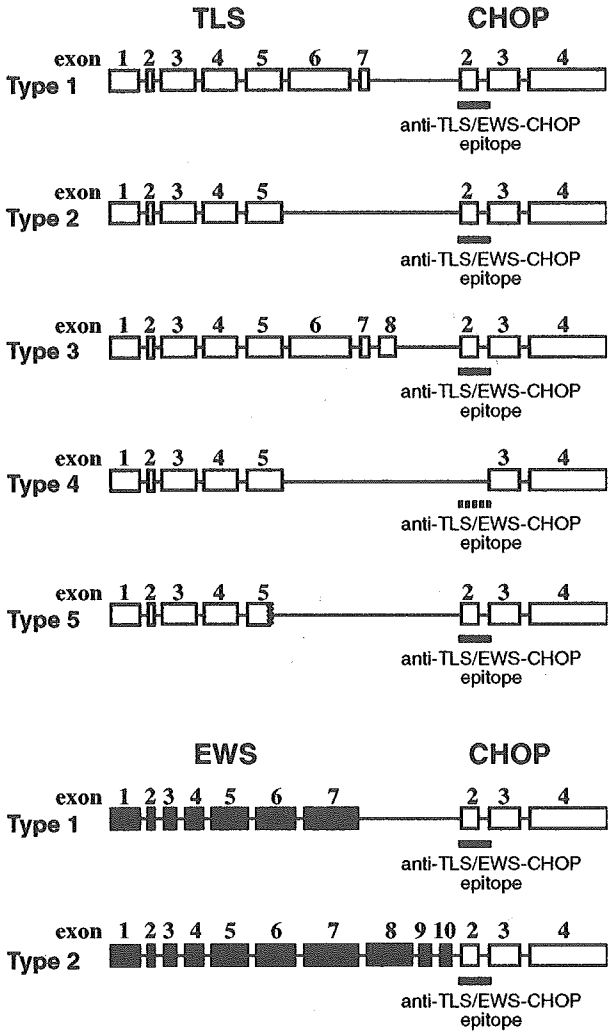

FIGURE 3. Structures of *TLS-CHOP* and *EWS-CHOP* fusion genes. The structure of each fusion gene is schematically represented. Gray, black, and open boxes represent exons of the *TLS*, *EWS*, and *CHOP* genes, respectively. The antibody recognition site is indicated as "anti TLS/EWS-CHOP epitope." Only *TLS-CHOP* type 4 does not have the epitope site.

scheduled expression of genes associated with adipocyte differentiation as a transcription factor.[11] However, we detected obvious positive staining for TLS-CHOP protein even in cells during mitosis (Fig. 2D). This observation suggests that the chimeric oncoproteins may affect some mitotic mechanisms, such as chromosome segregation, and induce chromosome instability. Elucidation of this hypothesis requires further studies, and we expect that the novel anti-TLS-CHOP antibody may be helpful to reveal the mechanism of MLS/RCLS oncogenesis. Nevertheless, we now introduce the TLS/EWS-CHOP specific antibody

TABLE 3. Variant form of *TLS-CHOP* and *EWS-CHOP*

		Panagopoulos *et al.*[17]	Knight *et al.*[6]	Kuroda *et al.*[8]	Panagopoulos *et al.*[16]	Hisaoka *et al.*[4]	Hosaka *et al.*[5]	This study	Total (cases)	Rate (%)
TLS-CHOP	Type 1	6		3		9	5		23	28.0
	Type 2	10	10	3		13	8	4	48	58.5
	Type 3			1			1		2	2.4
	Type 4						2		2	2.4
	Type 5						1		1	1.2
EWS-CHOP	Type 1				2		2		4	4.9
	Type 2						2		2	2.4
		16	10	7	2		21	4	82	100

(clone 14) as one of the best tools for diagnostic assays of MLS/RCLS.

REFERENCES

1. Antonescu CR, Elahi A, Humphrey M, et al. Specificity of TLS-CHOP rearrangement for classic myxoid/round cell liposarcoma: absence in predominantly myxoid well-differentiated liposarcomas. *J Mol Diagn.* 2000;2:132–138.
2. Antonescu CR, Kawai A, Leung DH, et al. Strong association of SYT-SSX fusion type and morphologic epithelial differentiation in synovial sarcoma. *Diagn Mol Pathol.* 2000;9:1–8.
3. Crozat A, Aman P, Mandahl N, et al. Fusion of CHOP to a novel RNA-binding protein in human myxoid liposarcoma. *Nature.* 1993;363:640–644.
4. Hisaoka M, Tsuji S, Morimitsu Y, et al. Detection of TLS/FUS-CHOP fusion transcripts in myxoid and round cell liposarcomas by nested reverse transcription-polymerase chain reaction using archival paraffin-embedded tissues. *Diagn Mol Pathol.* 1998;7:96–101.
5. Hosaka T, Nakashima Y, Kusuzaki K, et al. A novel type of EWS-CHOP fusion gene in two cases of myxoid liposarcoma. *J Mol Diagn.* 2002;4:164–171.
6. Knight JC, Renwick PJ, Cin PD, et al. Translocation t(12;16)(q13;p11) in myxoid liposarcoma and round cell liposarcoma: molecular and cytogenetic analysis. *Cancer Res.* 1995;55:24–27.
7. Kuroda M, Horiuchi H, Ono A, et al. Immunohistochemical study on the distribution of sarcoplasmic reticulum calcium ATPase in various human tissues using novel monoclonal antibodies. *Virchows Arch A Pathol Anat Histopathol.* 1992;421:527–532.
8. Kuroda M, Ishida T, Horiuchi H, et al. Chimeric TLS/FUS-CHOP gene expression and the heterogeneity of its junction in human myxoid and round cell liposarcoma. *Am J Pathol.* 1995;147:1221–1227.
9. Kuroda M, Ishida T, Takanashi M, et al. Oncogenic transformation and inhibition of adipocytic conversion of preadipocytes by TLS/FUS-CHOP type II chimeric protein. *Am J Pathol.* 1997;151:735–744.
10. Kuroda M, Sok J, Ron D. *The TLS-CHOP Oncogene and Human Liposarcoma.* Landes Bioscience: Georgetown TX; 1998.
11. Kuroda M, Wang X, Sok J, et al. Induction of a secreted protein by the myxoid liposarcoma oncogene. *Proc Natl Acad Sci USA.* 1999;96:5025–5030.
12. Ladanyi M, Bridge JA. Contribution of molecular genetic data to the classification of sarcomas. *Hum Pathol.* 2000;31:532–538.
13. Oikawa K, Ohbayashi T, Mimura J, et al. Dioxin stimulates synthesis and secretion of IgE-dependent histamine-releasing factor. *Biochem Biophys Res Commun.* 2002;290:984–987.
14. Oikawa K, Ohbayashi T, Mimura J, et al. Dioxin suppresses the checkpoint protein, MAD2, by an aryl hydrocarbon receptor-independent pathway. *Cancer Res.* 2001;61:5707–5709.
15. Panagopoulos I, Aman P, Mertens F, et al. Genomic PCR detects tumor cells in peripheral blood from patients with myxoid liposarcoma. *Genes Chromosomes Cancer.* 1996;17:102–107.
16. Panagopoulos I, Hoglund M, Mertens F, et al. Fusion of the EWS and CHOP genes in myxoid liposarcoma. *Oncogene.* 1996;12:489–494.
17. Panagopoulos I, Mandahl N, Ron D, et al. Characterization of the CHOP breakpoints and fusion transcripts in myxoid liposarcomas with the 12;16 translocation. *Cancer Res.* 1994;54:6500–6503.
18. Rabbitts TH. Chromosomal translocations in human cancer. *Nature.* 1994;372:143–149.
19. Rabbitts TH, Forster A, Larson R, et al. Fusion of the dominant negative transcription regulator CHOP with a novel gene FUS by translocation t(12;16) in malignant liposarcoma. *Nat Genet.* 1993;4:175–180.
20. Zinszner H, Albalat R, Ron D. A novel effector domain from the RNA-binding protein TLS or EWS is required for oncogenic transformation by CHOP. *Genes Dev.* 1994;8:2513–2526.
21. Zinszner H, Kuroda M, Wang X, et al. CHOP is implicated in programmed cell death in response to impaired function of the endoplasmic reticulum. *Genes Dev.* 1998;12:982–995.

The American Journal of Medicine (2005) 118, 782-786

ELSEVIER

THE AMERICAN JOURNAL of MEDICINE®

BRIEF OBSERVATION

Idiopathic retroperitoneal fibrosis associated with immunohematological abnormalities

Hisashi Oshiro, MD,[a,c] Yoshiro Ebihara, MD,[a] Hiromi Serizawa, MD,[a] Toru Shimizu, MD,[a] Shinichi Teshima, MD,[b] Masahiko Kuroda, MD,[a] Motoshige Kudo, MD[a]

[a]*Department of Pathology, Tokyo Medical University, and*
[b]*Division of Pathology, Fraternity Memorial Hospital, Tokyo; and the*
[c]*Department of Pathology, Yokohama City University School of Medicine, Kanagawa, Japan.*

Idiopathic retroperitoneal fibrosis is characterized by the deposition of dense fibrous connective tissue and varying degrees of lymphoid cell infiltration.[1] Some descriptions of this disease also refer to the presence of distorted plasma cells and to nuclear irregularities and clonal gene rearrangement in the lymphoid cells.[2,3] Reports of the incidence of malignant lymphoma, following an initial diagnosis of idiopathic retroperitoneal fibrosis and associated conditions,[4-8] suggest that these sclerosing entities should perhaps be classified as lymphoid dyscrasia, which may be predisposed to forming low grade malignant lymphomas.[3] The aim of this study was to further investigate immunohematological abnormalities in cases of idiopathic retroperitoneal fibrosis.

Methods

The diagnostic criteria that we used for characterizing a case of idiopathic retroperitoneal fibrosis were as follows: the lesions could be histologically characterized by dense fibrous connective tissue with varying degrees of polymorphous inflammatory cell infiltration[9] and there was neither a history nor any indication of a probable cause of secondary retroperitoneal fibrosis, for example, metastatic carcinoma, malignant lymphoma, granulomatous disorders, established connective-tissue diseases, or use of certain drugs such as methysergide or bromocriptine.[10] If fibrosclerotic lesions were found at an additional site from the retroperitoneum, these lesions were also included in this study as cases of multifocal fibrosclerosis or systemic idiopathic fibrosis.[11-13] In order to exclude cases of malignancy during the initial diagnoses, a 4-year minimum follow-up period or an autopsy was required in each case.

Five cases, treated in our hospitals between 1984 and 1998, were reviewed and determined as having fulfilled the diagnostic criteria. A total of 7 tissue specimens, fixed in formalin and embedded in paraffin, were obtained from these cases and used in this study.

Immunohistochemical studies were performed by an automated immunostaining system (Autostainer; Dako; Copenhagen, Denmark). The monoclonal antibody panel included CD3 (PC3/188A; Dako), CD10 (SS2/36; Dako), CD20/cy (L26; Dako), CD45RO (UCHL1; Dako), CD68 (PG-M1; Dako), CD79a (JCB117; Dako), kappa light chains (R10-21-F3; Dako), lambda light chains (N10/2, Dako), bcl-2 (124; Dako), and bcl-10 (151; Zymed Laboratories; San Francisco, Calif). Nuclear bcl-10 expression was evaluated as previously described.[14] In addition, CD3, lambda light chain, and kappa light chain polyclonal antibodies (Dako) were used. In situ hybridizations for Epstein-Barr virus-encoded small RNA were performed using the EBER PNA Probe and PNA in situ hybridization Detection Kit (Dako).

Supported in part by a Grant-in-Aid for Medical Research from the Tokyo Medical University Cancer Center, which had no role in the study design, data collection, data analysis, data interpretation or writing of this report.

Requests for reprints should be addressed to Hisashi Oshiro, MD, Department of Pathology, Yokohama City University School of Medicine, 3-9 Fukuura, Kanazawa-ku, Yokohama-shi, Kanagawa 236-0004, Japan.

E-mail address: oshiroh@yokohama-cu.ac.jp.

0002-9343/$ -see front matter
doi:10.1016/j.amjmed.2005.02.004

We performed polymerase chain reaction (PCR) analysis to investigate lymphoid clonality using DNA templates, obtained in triplicate, from the 7 tissue specimens. Each of the DNA templates were determined to be of sufficient concentration (more than 50 pg/μL) and sample quality for these analyses, following successful β-globin gene amplification.[15,16] Immunoglobulin heavy chain gene rearrangements were examined by semi-nested PCR, using the primers FR3A, LJH, and VLJH.[17] T-cell receptor-β gene rearrangements were examined by standard PCR using primers Dβ2 and Jβ2.[18] We used 12 samples without lymphomatous lesions as negative controls for PCR, and 3 samples of B-cell lymphoma as positive controls for immunoglobulin heavy chain gene rearrangement. In addition, one sample of a peripheral T-cell lymphoma was used as a positive control for T-cell receptor-β gene rearrangement.

PCR were carried out in a general reaction mixture using Taq polymerase (TaKaRa Ex Taq; TaKaRa; Shiga, Japan) and amplified products were analyzed on 4% agarose gels. For the evaluation of monoclonality in each sample, one or two distinct sharp bands between an appropriate base pair were considered positive, whereas either broad smears, multiple nondiscrete bands, or a lack of amplification were considered negative.[17,18] To confirm the monoclonality of our PCR products, each fragment was sub-cloned and sequenced.[19]

Results

All 5 cases of idiopathic retroperitoneal fibrosis examined in this study demonstrated constitutional symptoms (Table 1). Dysproteinemia was evident in 4 cases, from which 2 (cases 1 and 4) showed polyclonal gammopathy and 2 (cases 3 and 5) demonstrated IgA and IgG elevation. Lymphadenopathy was observed in 3 cases (cases 1, 2, and 5) and multifocal fibrosclerotic lesions were also detected in 3 cases (cases 1, 3, and 4). Gallium scintigraphy was performed in 4 cases (cases 1, 2, 3, and 5), and 2 of these (cases 3 and 5) showed accumulation. Autoantibodies were positive in 2 cases (cases 1 and 3), but there was no clinicopathological evidence of known connective-tissue diseases in these cases. In addition, there was no evidence of thyroiditis, aneurysm, or severe atherosclerosis in any of these 5 cases. Three of the 4 cases receiving oral prednisolone showed reductions in retroperitoneal fibrosis or improvement of their symptoms (cases 1, 2, and 3), but the remaining individual (case 5) died of Stevens-Johnson syndrome.

Histopathological examination of the tissue specimens confirmed the diagnosis of idiopathic retroperitoneal fibrosis or idiopathic fibrosclerotic disorder (Table 2), and all demonstrated dense fibrous connective tissue with compound foci of lymphocytes, plasma cells, histiocytes, and granulocytes, sometimes associated with vague lymph follicles. Furthermore, fibroblastic proliferation was lacking in any of the cases, which distinguished them from typical fibromatosis. Vasculitic changes were found in 4 specimens, but only a few vessels were involved, and no amyloidosis was evident in any of the specimens. Immunohistochemical studies also confirmed the presence of polyclonal lymphocytic infiltration with sparsely populated scanty clusters of small lymphocytes, characterized by cleaved nuclear membranes. Nuclear bcl-10 expression was observed in these infiltrating lymphocytes in 4 of the 7 specimens. Results of in situ hybridization for Epstein-Barr virus were negative in all specimens.

Each of the tissue specimens demonstrated clonal immunoglobulin heavy chain gene rearrangement (Figure), but none showed clonal T-cell receptor-β gene rearrangement, and this was confirmed by the controls. These reactions were performed in triplicate, giving identical results. Sequencing results were as follows: specimen 1-a: ACACG GCCGTGTATTACTGTGCGAGATTGGCTGGAGCCAC CTCTGGGGCTTTTGATTTCTGGGGCCAAGGTACCC TGGTCAC; 1-b: ACACGGCCGTGTATTACTGTGCGC CTCTAAGGGGCCTCTGGGATTTTTATCGCACGAGA CTGGGGCCAAGGTACCCTGGTCAC; 1-c: ACACG GCCGTGTATTACTGTGCGAGACCCGCCGCCATCTG GGGCCAAGGTACCCTGGTCAC; 2: ACACGGCCGTG TATTACTGTGCGAGAGAGAAGCGGTATAACTGGA ACTACCCGGCGGGTAGTATGGACGTCTGGGGCCAA GGTACCCTGGTCAC; 3: ACACGGCCGTGTATTACT GTACCACAGAGGAGGTGATGTATGGTTCGGGGAGT CATCGTGCTTCTGACTACTGGGGCCAAGGTACCC TGGTCAC; 4: ACACGGCCGTGTATTACTGTGC GA GGGCAAGACTCCCTTACTACTCCTACGCTATGGAC GTCTGGGGCCAAGGTACCCTGGTCAC; and 5: ACA CGGCCGTGTATTACTGTGCGAGAATCTGGAACCTC ACCTCATCCCCTGGGGCCAAGGTACCCTGGTCAC.

Discussion

Our findings can be summarized as follows: each of our 5 cases of idiopathic retroperitoneal fibrosis demonstrates constitutional symptoms, vasculitic changes are evident in 4 cases, all cases demonstrated either monoclonal or oligoclonal immunoglobulin heavy chain gene rearrangement, and the nuclear bcl-10 expression of lymphoid cells was identified in 3 cases.

The causes of idiopathic retroperitoneal fibrosis are still somewhat obscure, although an autoimmune-mediated or vasculitic etiology has been hypothesized.[10,12,20] There are some reported associations between autoimmune disease and immunoglobulin heavy chain gene monoclonality, but the detection of clonality does not necessarily allow for a diagnosis of malignant lymphoma.[21] In addition, cases showing favorable responses to immunosuppressive therapy may support the immune-mediated etiology.[22] However, only about 10% of cases harbor autoantibodies, and vasculitis is not a specific feature of this disease.[23] Because monoclonal or oligoclonal immunoglobulin heavy chain

Table 1 Results of clinical findings of 5 cases with idiopathic retroperitoneal fibrosis

Case no.	Age (year)/Sex	Clinical manifestations	Dysproteinemia	Details of fibrosclerotic lesion	Therapy	Follow-up and outcome
1	66/man	Chronic bronchitis, hilar and cervical lymphadenopathy (reactive follicular hyperplasia), cryptogenic cholangitis, renal dysfunction, right lower extremity edema, bilateral submandibular gland enlargement, cryptogenic diplopia, right hydronephrosis, elevated erythrocyte sedimentation rate, perinuclear anticytoplasmic antibody (+)	Polyclonal gammopathy 24.6% (7.8–20.9) IgG elevation 2700 mg/dL (885–1822)	A bronchial mass (about 4 × 3 mm) A retroperitoneal mass (about 55 × 45 × 30 mm) A mass of the bilateral submandibular gland (about 30 mm in diameter)	Prednisolone	No malignant change for 144 months, with disappearance of diplopia
2	59/woman	Intermittent abdominal pain, slight malaise, anemia, right lower extremity edema, bilateral submandibular lymph node swelling, anemia, right hydronephrsosis, elevated C-reactive protein level	Unclear	A retroperitoneal mass (about 50 × 50 × 40 mm)	Prednisolone	No malignant change for 56 months, with disappearance of retroperitoneal mass
3	58/man	Left lower extremity edema, back pain on the left side, claudication, left inguinal mass, anemia, left hydronephrosis, rheumatoid factor (+), antinuclear antibody (+), antiribonucleoprotein antibody (+), elevated C-reactive protein level and erythrocyte sedimentation rate	IgA elevation 489 mg/dL (114–470)	A retroperitoneal mass (about 70 × 50 × 40 mm) A left inguinal mass (about an index finger size)	Prednisolone	No malignant change for 56 months, with disappearance of retroperitoneal mass (about 140 × 110 × 37 mm)
4	83/woman	Liver dysfunction, malaise, appetite loss, weight loss (10 kg reduction for 3 months), anemia, bleeding rectal ulcer, elevated C-reactive protein level and erythrocyte sedimentation rate	Polyclonal gammopathy 41.2%	Diffusely expansive bilateral perirenal fibrosclerotic tissue, invading into renal cortex and pelvis A mesorectal mass (about 35 mm)	None	Died of hemorrhage from a rectal ulcer (autopsied case)
5	44/woman	Recurrent stomatitis, leukocytopenia, fever of unknown etiology, appetite loss, bilateral pseudomembranous conjunctivitis, genital ulcer, blister, systemic lymphadenopathy, elevated C-reactive protein level	IgG elevation 1890 mg/dL	A retroperitoneal mass (about 140 × 110 × 37 mm)	Prednisolone	Died of Stevens-Johnson syndrome after 3 months (autopsied case)

Table 2 Results of histopathology, immunohistochemistry, in situ hybridization, and gene rearrangement

Specimen no.*	Site	Histopathological diagnosis	Vasculitic changes	Immunohistochemistry				In situ hybridization for Epstein-Barr virus	Gene rearrangement¶	
				B-cell/T-cell ratio†	κ/λ ratio‡	Bcl-10§			Immunoglobulin heavy chain	T-cell receptor-β
1-a	Retroperitoneum	Idiopathic retroperitoneal fibrosis	Present	1/1	1/1	(−)		(−)	(+)	(−)
1-b	Bronchial mucosa	Idiopathic fibrosclerotic disorder	Uncertain	1/1	2/1	(+)		(−)	(+)	(−)
1-c	Submandibular gland	Idiopathic fibrosclerotic disorder	Uncertain	1/1	1/1	(+)		(−)	(+)	(−)
2	Retroperitoneum	Idiopathic retroperitoneal fibrosis	Present	1/1	1/1	(+)		(−)	(+)	(−)
3	Retroperitoneum	Idiopathic retroperitoneal fibrosis	Present	1/1	1/1	(+)		(−)	(+)	(−)
4	Retroperitoneum	Idiopathic retroperitoneal fibrosis	Present	1/1	1/1	(−)		(−)	(+)	(−)
5	Retroperitoneum	Idiopathic retroperitoneal fibrosis	Uncertain	1/1	1/1	(−)		(−)	(+)	(−)

*The numeral represents the case number and the letter denotes a different specimen derived from the same case.
†B-cell/T-cell ratio denotes the proportion of B-cells and T-cells in the lesion.
‡κ/λ ratio denotes the proportion of kappa-light-chain positive cells and lambda-light-chain positive cells in the lesion.
§Positive results are defined as nuclear bcl-10 expression of lymphoid cells.
¶Positive results are defined as clonal gene rearrangement.

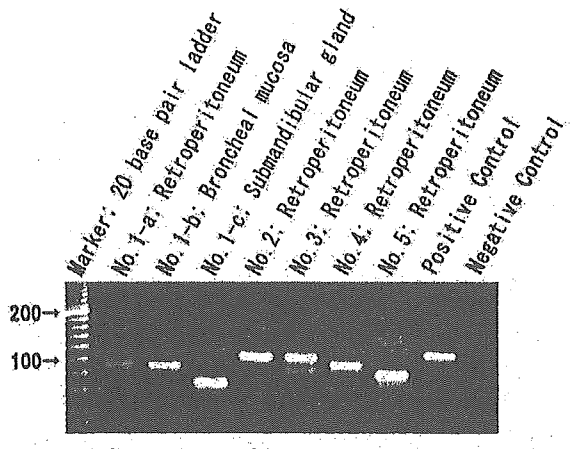

Figure 1 PCR analyses of immunoglobulin heavy chain gene rearrangements, showing clonal gene rearrangements in all of the cases with idiopathic retroperitoneal fibrosis.

gene rearrangement and fibrosis were found to coexist in all of the cases that we examined, we propose that either monoclonal or oligoclonal B-cell expansion might contribute to the pathogenesis of the fibrotic process. Moreover, one might assume that all cases were examples of lymphoma de novo, as malignant lymphoma can present as lesions characterized by considerable sclerosis. However, diagnosis should be based on generally accepted criteria,[24] and our diagnosis was confirmed by an appropriate level of material with a minimum of a 4-year follow-up and autopsy.

Reports of the occurrence of malignant lymphoma, particularly B-cell malignancies, in follow-ups of patients diagnosed with benign retroperitoneal fibrosis are noteworthy and need further discussion.[4-8,23,25] Our finding of clonal immunoglobulin heavy chain gene rearrangement raises the possibility that this disease may have a potential predisposition to B-cell lymphoma. An example of this is an autoimmune disease or *Helicobacter pylori*-associated chronic gastritis in which the lesion has a clonal B-cell population, despite the absence of both histological and clinical evidence of malignant lymphoma but the risk of overt malignant lymphoma.[21,26]

Nuclear bcl-10 expression has been demonstrated in neoplastic lymphoid cells,[14,27] but the sparse distribution of lymphoid cells expressing nuclear bcl-10 in our study does not seem to be consistent with a diagnosis of malignant lymphoma. We speculate, therefore, that bcl-10 expression may be associated with clonal lymphoid expansion or lymphocyte survival signaling[14,28,29] through the activation of the NF-kappaB pathway.[30] Alternatively, it may represent a process that mediates multiple signaling pathways related to fibroblast growth factor regulation and collagen synthesis,[31,32] although proof of this was not within the scope of this study.

Chim et al previously reported a case of lymphoma that mimicked idiopathic retroperitoneal fibrosis and stressed the importance of clonality studies.[25] The initial diagnosis of their case was idiopathic retroperitoneal fibrosis, but this case developed diffuse large B-cell lymphoma within 8

years. Further investigations are desirable in rare cases of long-term indolent lymphoma, but we predict that their case did not mimic idiopathic retroperitoneal fibrosis but actually presented with some of the features of lymphoid abnormalities in idiopathic retroperitoneal fibrosis. This would likely result in the impression that there is no absolute evidence to distinguish the initial retroperitoneal lesion they investigated from the lesions described in the literature as idiopathic retroperitoneal fibrosis.[1-3,9-13,20,23]

In conclusion, immunohematological abnormalities demonstrated in idiopathic retroperitoneal fibroses and their related conditions suggest that, at least in some cases, these entities might be considered to be part of the spectrum of lymphoid dyscrasia.

Acknowledgment

We are indebted to Professor Kiyoshi Mukai of the Department of Pathology of Tokyo Medical University and Dr. Akihide Ryo of the Department of Pathology of Yokohama City University School of Medicine for useful discussions. We also thank Professor J. Patrick Barron of the International Medical Communications Center of Tokyo Medical University for his review of this manuscript and Mr. Koji Fujita of the Department of Pathology of Tokyo Medical University for his technical assistance.

References

1. Ormond JK. Bilateral ureteral obstruction due to envelopment and compression by an inflammatory retroperitoneal process. *J Urol.* 1948; 59:1072–1079.
2. Osborne BM, Butler JJ, Bloustein P, Sumner G. Idiopathic retroperitoneal fibrosis (sclerosing retroperitonitis). *Hum Pathol.* 1987;18:735–739.
3. Dent GA, Baird DB, Ross DW. Systemic idiopathic fibrosis with T-cell receptor gene rearrangement. *Arch Pathol Lab Med.* 1991;115: 80–83.
4. Kiely JM, Wagoner RD, Holley KE. Renal complications of lymphoma. *Ann Intern Med.* 1969;71:1159–1175.
5. Hurley BP, Macarthur EB, Utley GL. Retroperitoneal fibrosis, methysergide and malignant lymphoma. *Aust N Z J Med.* 1978;8:417–419.
6. Man KM, Dreget A, Keeffe EB, et al. Primary sclerosing cholangitis and Hodgkin's disease. *Hepatology*1993;18:1127–1131.
7. Vigouroux C, Escourolle H, Mosnier-Pudar H, et al. Riedel's thyroiditis and lymphoma: diagnostic difficulties. *Presse Med.* 1996;25:28–30.
8. García JF, Sánchez E, Lloret E, et al. Crystal-storing histiocytosis and immunocytoma associated with multifocal fibrosclerosis. *Histopathology.* 1998;33:459–464.
9. Rosai J. *Ackerman's Surgical Pathology*, 8th edn. vol 2. New York, New York: Mosby; 1996: 2155–2156.
10. Kottra JJ, Dunnick NR. Retroperitoneal fibrosis. *Radiol Clin North Am.* 1996;34:1259–1275.
11. Comings DE, Skubi KB, Van Eyes J, Motulsky AG. Familial multifocal fibrosclerosis: findings suggesting that retroperitoneal fibrosis, mediastinal fibrosis, sclerosing cholangitis, Riedel's thyroiditis, and pseudotumor of the orbit may be different manifestations of a single disease. *Ann Intern Med.* 1967;66:884–892.
12. Mitchinson MJ. The pathology of idiopathic retroperitoneal fibrosis. *J Clin Pathol.* 1970;23:681–689.
13. Hamano H, Kawa S, Ochi Y, et al. Hydronephrosis associated with retroperitoneal fibrosis and sclerosing pancreatitis. *Lancet.* 2002;359: 1403–1404.
14. Ye H, Dogan A, Karran L, Willis TG, et al. BCL10 expression in normal and neoplastic lymphoid tissue: nuclear localization in MALT lymphoma. *Am J Pathol.* 2000;157:1147–1154.
15. Elenitoba-Johnson KS, Bohling SD, Mitchell RS, et al. PCR analysis of the immunoglobulin heavy chain gene in polyclonal processes can yield pseudoclonal bands as an artifact of low B cell number. *J Mol Diagn.* 2000;2:92–96.
16. Saiki RK, Gelfand DH, Stoffel S, et al. Primer-directed enzymatic amplification of DNA with a thermostable DNA polymerase. *Science.* 1988;239:487–491.
17. Achille A, Scarpa A, Montresor M, et al. Routine application of polymerase chain reaction in the diagnosis of monoclinality of B-cell lymphoid proliferations. *Diagn Mol Pathol.* 1995;4:14–24.
18. Diss TC, Watts M, Pan LX, et al. The polymerase chain reaction in the demonstration of monoclonality in T cell lymphomas. *J Clin Pathol.* 1995;48:1045–1050.
19. Ausubel FM, Brent R, Kingston RE, et al., eds. *Current Protocols in Molecular Biology*, vol. 1. New York, New York: John Wiley & Sons; 2001.
20. Vaglio A, Corradi D, Manenti L, et al. Evidence of autoimmunity in chronic periaortitis: a prospective study. *Am J Med.* 2003;114: 454–462.
21. Fishleder A, Tubbs R, Hesse B, Levine H. Uniform detection of immunoglobulin-gene rearrangement in benign lymphoepithelial lesions. *N Engl J Med.* 1987;316:1118–1121.
22. Marcolongo R, Matteo Tavolini IM, Laveder F, et al. Immunosuppressive therapy for idiopathic retroperitoneal fibrosis: a retrospective analysis of 26 cases. *Am J Med.* 2004;116:194–197.
23. Glikeson GS, Allen NB. Retroperitoneal fibrosis: a true connective tissue disease. *Rheum Dis Clin North Am.* 1996;22:23–38.
24. Jaffe ES, Harris NL, Stein H, Vardiman JW. *Pathology and Genetics of Tumors of Haematopoietic and Lymphoid Tissues. World Health Organization Classification of Tumors.* Lyon, France: IARC Press; 2001.
25. Chim CS, Liang R, Chan AC. Sclerosing malignant lymphoma mimicking idiopathic retroperitoneal fibrosis: importance of clonality study. *Am J Med.* 2001;111:240–241.
26. Zucca E, Bertoni F, Roggero E, et al. Molecular analysis of the progression from *Helicobacter pylori*-associated chronic gastritis to mucosa-associated lymphoid-tissue lymphoma of the stomach. *N Engl J Med.* 1998;338:804–810.
27. Maes B, Demunter A, Peeters B, De Wolf-Peeters C. BCL10 mutation does not represent an important pathogenic mechanism in gastric MALT-type lymphoma, and the presence of the API2-MLT fusion is associated with aberrant nuclear BCL10 expression. *Blood.* 2002;99: 1398–1404.
28. Ruland J, Duncan GS, Elia A, et al. Bcl10 is a positive regulator of antigen receptor-induced activation of NF-kappaB and neural tube closure. *Cell.* 2001;104:33–42.
29. Patke A, Mecklenbrauker I, Tarakhovsky A. Survival signaling in resting B cells. *Curr Opin Immunol.* 2004;16:251–255.
30. Zhou H, Wertz I, O'Rourke K, et al. Bcl10 activates the NF-kappaB pathway through ubiquitination of NEMO. *Nature.* 2004;427: 167–171.
31. Bushdid PB, Chen CL, Brantley DM, et al. NF-kappaB mediates FGF signal regulation of msx-1 expression. *Dev Biol.* 2001;237:107–115.
32. Tang JB, Xu Y, Ding F, Wang XT. Tendon healing in vitro: promotion of collagen gene expression by bFGF with NF-kappaB gene activation. *J Hand Surg.* 2003;28:215–220.

Available online at www.sciencedirect.com
SCIENCE DIRECT®
Cancer Letters 221 (2005) 21–28
CANCER Letters
www.elsevier.com/locate/canlet

Effects of 3-methylcholanthrene on the transcriptional activity and mRNA accumulation of the oncogene *hWAPL*

Masahiko Kuroda[a,b,c,*], Kosuke Oikawa[a,b,c], Keiichi Yoshida[a,c], Aya Takeuchi[d], Masaru Takeuchi[d], Masahiko Usui[d], Akihiro Umezawa[c,e], Kiyoshi Mukai[a]

[a]*Department of Pathology, Tokyo Medical University, 6-1-1 Shinjuku, Shinjuku-ku, Tokyo 160-8402, Japan*
[b]*CREST Research Project, Japan Science and Technology Corporation, 4-1-6 Kawaguchi, Saitama 332-0012, Japan*
[c]*Shinanomachi Research Park, Keio University, 35 Shinanomachi, Shinjuku-ku, Tokyo 160-8582, Japan*
[d]*Department of Ophthalmology, Tokyo Medical University, 6-7-1 Nishi-shinjuku, Shinjuku-ku, Tokyo 160-0023, Japan*
[e]*National Research Institute for Child Health and Development, 3-35-31 Taishido, Setagaya-ku, Tokyo 154-8567, Japan*

Received 28 April 2004; received in revised form 26 July 2004; accepted 5 August 2004

Abstract

hWAPL is a human oncogene associated with uterine cervical cancer. Here, we demonstrate that *hWAPL* transcription is induced by 3-methylcholanthrene (3-MC) in the cervical carcinoma-derived cell line SiHa. *hWAPL* transcription was analyzed with evaluation of the mRNA and heterogeneous nuclear RNA (hnRNA) levels by quantitative real time PCR analysis. Flow cytometric analysis suggested that the alteration of *hWAPL* mRNA levels is independent of cell cycle profile. We also found that DMSO and some components of FBS affect *hWAPL* transcription. Interestingly, when the aryl hydrocarbon receptor (AhR) function was inhibited by α-naphthoflavone (ANF), the induction of *hWAPL* transcription by 3-MC was greater than that in AhR-functioning normal cells. These observations suggest that there are complex mechanisms regulating the transcription of *hWAPL*. Furthermore, mRNA level of a mouse homolog of *hWAPL* in mouse uterus was induced by 3-MC injection into the abdominal cavity. Thus, some effects from 3-MC exposure on uterus may be mediated by the unscheduled overexpression of *hWAPL*.

Keywords: 3-Methylcholanthrene (3-MC); hWAPL; Uterine cervical cancer; Aryl hydrocarbon receptor (AhR); α-naphthoflavone (ANF)

1. Introduction

Previously, we have isolated and characterized a novel human gene termed *hWAPL* [1]. Our initial observations suggested that *hWAPL* expression is associated with uterine cervical cancer, although the mechanism was not clear. *hWAPL* is the human homolog of the *wings apart-like* (*wapl*) gene in

* Corresponding author. Address: Department of Pathology, Tokyo Medical University, 6-1-1 Shinjuku, Shinjuku-ku, Tokyo 160-8402, Japan. Tel.: +81 3 3351 6141x425; fax: +81 3 3352 6335.
E-mail address: kuroda@tokyo-med.ac.jp (M. Kuroda).

0304-3835/$ - see front matter © 2004 Elsevier Ireland Ltd. All rights reserved.
doi:10.1016/j.canlet.2004.08.006

Drosophila melanogaster. The protein encoded by *wapl* controls heterochromatin organization and was identified as a modifier of both PEV and chromosome inheritance [2,3]. Thus, hWAPL is also expected to be involved in heterochromatin maintenance and epigenetic control.

Polycyclic aromatic hydrocarbons (PAHs) are carcinogenic and immunotoxic chemicals widely distributed in the environment [4]. 3-Methylcholanthrene (3-MC) is one of the most toxic and the best-studied compounds in the PAHs. Most of the toxic effects of PAHs are mediated by the aryl hydrocarbon receptor (AhR) [5]. When PAHs bind to the AhR, the ligated AhR translocates from the cytoplasm to the nucleus where it switches its partner molecule from heat shock protein 90 kD (Hsp90) to the aryl hydrocarbon receptor nuclear translocator (Arnt) [6]. The resulting AhR/Arnt heterodimer binds a specific DNA sequence, designated xenobiotic responsive element (XRE), in the promoter region of target genes to enhance their expression [6]. On the other hand, several studies have suggested the existence of AhR independent pathways for PAH toxicity [7,8]. In all cases, many of the putative target genes responsible for the toxicity symptoms have yet to be identified.

In the present study, we demonstrate that *hWAPL* is a target gene of 3-methylcholanthrene. The results suggest that carcinogenesis by 3-MC may involve alterations of *hWAPL* gene expression.

2. Materials and methods

2.1. Chemicals

3-Methylcholanthrene (Sigma-Aldrich Japan, Tokyo, Japan) was prepared in dimethylsulfoxide (DMSO) for cultured cells and in olive oil for treatment of mice. Aphidicolin (Wako Pure Chemical Industries, Ltd, Osaka, Japan), Nocodazole (Sigma Chemical Co., St Louis, MO) and α-naphthoflavone (Sigma) were prepared in DMSO.

2.2. Cell cultures

The human uterine cervical carcinoma-derived cell lines, SiHa, CaSki and HeLa cells, were obtained from American Type Culture Collection (ATCC), and grown in DMEM (Sigma) supplemented with 10% fetal bovine serum (FBS) (Trace Scientific Ltd, Melbourne, Australia) at 37 °C in a 5% CO_2 environment. Where indicated, SiHa cells were grown in DMEM supplemented with 10% charcoal/dextran treated FBS (CTF) (Biosource, Rockville, MD) or 0.4% (w/v) bovine serum albumin (BSA) (Trace) instead of FBS.

2.3. Immunoblot analysis

Protein samples were prepared as previously described [9]. Immunoblot analysis was performed as previously described [1].

2.4. Flow cytometric analysis

To determine cell cycle profiles, cells at different time points were harvested, washed, and fixed with a solution containing 70% ethanol and 30% PBS. After incubation overnight at 4 °C, cells were suspended in staining buffer (propidium iodide, 50 μg/ml; RNaseA, 0.1%; glucose, 1 mg/ml in PBS). Then, after incubation for 30 min at room temperature, the cells were analyzed with a FACS Vantage flow cytometer using the Cell Quest acquisition and analysis program (BD Biosciences, San Jose, CA).

2.5. Animals and treatment

C57/BL6 female mice (6 weeks old) were purchased from Oriental Yeast Co., Ltd (Tokyo, Japan). The mice received a single intraperitoneal injection of 1 ml of olive oil containing 3-MC at a dose of 80 mg/kg of body mass. The control mice were injected with olive oil alone. Uterus samples were harvested 24 and 48 h after injection and subjected to real time PCR analysis.

2.6. RNA isolation and quantitative real time PCR

First strand cDNA synthesis was performed as described [10] using M-MLV Reverse transcriptase (Invitrogen Japan, Tokyo, Japan) with Oligo $(dT)_{17}$ (for Figs. 1–3 and 6) or Random Primers (Invitrogen) (for Figs. 4 and 5).

Real time PCR analysis for *hWAPL* and human β-*actin* mRNAs was performed as described [1]

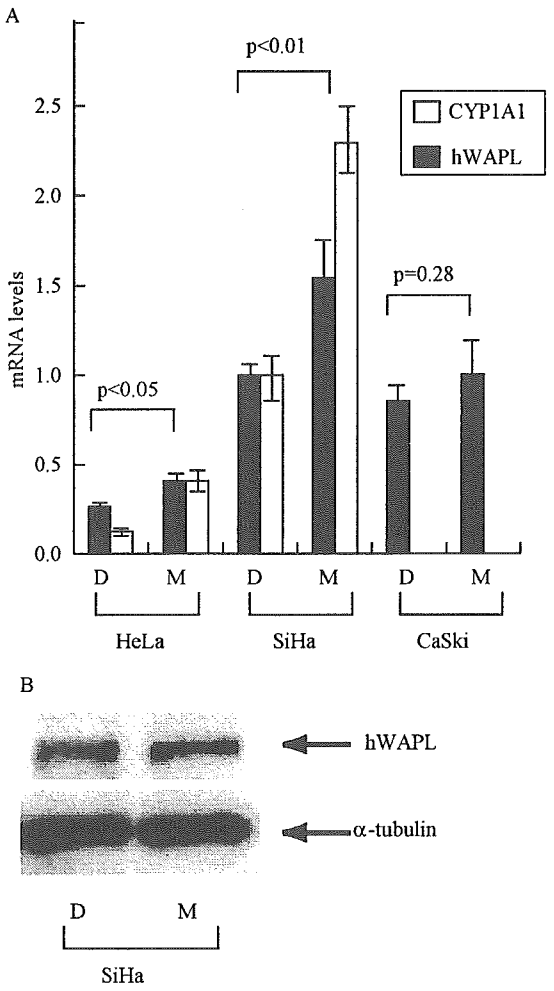

Fig. 1. Effects of 3-MC on *hWAPL* expression in the human cervical cancer-derived cell lines. D, DMSO alone; M, 3-MC. (A) HeLa, SiHa and CaSki cells were treated with 0.1% DMSO alone or 1 μM of 3-MC for 6 h. Then, the *hWAPL* and *CYP1A1* mRNA levels in the cells were evaluated by quantitative real time PCR analysis. Data were normalized to the mRNA levels of SiHa cells treated with DMSO alone that was arbitrarily set to 1 in the graphical presentation. *Bars, s.e.* (B) SiHa cells were treated with 0.1% DMSO alone or 1 μM 3MC for 6 h, and then the protein samples were prepared and subjected to western blotting analysis. α-tubulin was also shown as a loading control.

except for the 40 PCR cycles at 95 °C for 3 s and 68 °C for 30 s. Real Time PCR analysis for human *CYP1A1* mRNA and *hWAPL* hnRNA was also performed with the same PCR protocol. The nucleotide sequences of primers specific for human *CYP1A1* mRNA were previously described [11]. Primers specific for *hWAPL* hnRNA are 5′-GAGATTACACCACTGCACTCC-3′ and 5′-TTGCTCCCACTTACTATGGCC-3′. For mouse cDNAs, we used primers specific for the mouse homolog of *hWAPL* mRNA, 5′-ACCTGGTGGAGTATAGTGCCC-3′ and 5′-TGGCAGAGACACCCAAGAAGC-3′ (The nucleotide sequences were obtained from mKIAA0261 in Database), mouse β-*actin* mRNA, 5′-AGCCTTCCTTCTTGGGTATGG-3′ and 5′-CACTTGCGGTGCACGATGGAG-3′, and mouse *CYP1A1* mRNA, 5′-TTTGGTTTGGGCAAGCGA-3′ and 5′-GTCTAAGCCTGAAGATGC-3′. Reaction mixtures were denatured at 95 °C for 30 s then subjected to 40 PCR cycles at 95 °C for 3 s, 68 °C for 30 s, and 86 °C for 6 s for mouse *WAPL* mRNA, and at 95 °C for 3 s, 68 °C for 30 s, and 85 °C for 6 s for mouse β-*actin* and *CYP1A1* mRNAs, respectively. *hWAPL, mouse WAPL* and human and mouse *CYP1A1* mRNA levels and *hWAPL* hnRNA level were normalized to human and mouse β-*actin* signals, respectively. The absence of PCR products after the PCR on non-reverse-transcribed total RNA served as a routine check for contaminating genomic DNA. We performed the experiments to determine mRNA and hnRNA levels in triplicate.

The data were analyzed using Student's-*t* test, and $Ps < 0.05$ were considered to indicate significant differences.

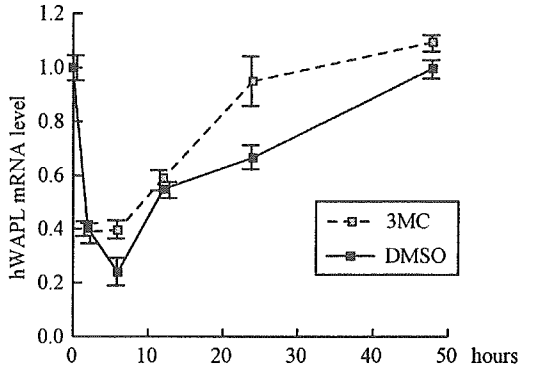

Fig. 2. Kinetics of *hWAPL* mRNA levels in SiHa cells at several time points after treatment with DMSO alone or 1 μM of 3-MC. The *hWAPL* mRNA levels in the cells were evaluated by quantitative real time PCR analysis. Data were normalized to the mRNA level at 0 h that was arbitrarily set to 1 in the graphical presentation. *Bars, s.e.*